

Advances in Functional Metal-Organic Frameworks Based On-Demand Drug Delivery Systems for Tumor Therapeutics

Bhanu Nirosha Yalamandala, Wei-Ting Shen, Sheng-Hao Min, Wen-Hsuan Chiang, Shing-Jyh Chang, and Shang-Hsiu Hu*


Dual on-demand delivery of therapeutic cargos and energy by transporters can latently mitigate side effects and provide the unique aspects required for precision medicine. To achieve this goal, metal-organic frameworks (MOFs), hybrid materials constructed from metal ions and polydentate organic linkers, have attracted attention for controlled drug release and energy delivery in tumors. With appropriate characteristics such as tunable pore size, high surface area, and tailorable composition, therapeutic agents (drug molecules or responsive agents) can be effectively encapsulated in MOFs. Based on their intrinsic properties, many physically or chemically responsive agents are able to achieve precise on-demand drug release and energy generation (thermal or dynamic therapy) using MOFs (as energy absorbers). Herein, the results obtained with various stimuli-responsive MOFs (including materials from the Institute Lavoisier [MIL], zeolitic imidazolate frameworks [ZIFs], MOFs from the University of Oslo [UiO], and other MOFs) used for tumor suppression are summarized. Furthermore, with the appropriate stimulus, catalytic therapy (caused by the Fenton reaction induced by MOFs) can be provided via the utilization of existing high levels of H_2O_2 in cancer cells, which potentially elicits immune responses. In addition, the issues impeding clinical translation are also discussed, including the need to overcome tumor heterogeneity and to recognize the innate immune system and possible effects. As the references reveal, additional comprehensive strategies and studies are needed to enable broad applications and potent translational developments.

therapeutic agents and tumor-treating modalities.^[1,2] In the past few decades, numerous nanoscale DDSs have been developed to reduce side effects, enhance therapeutic efficacy, and provide controlled drug release.^[3] Some of them have been approved by the Food and Drug Administration (FDA) and used in clinical tumor treatments, including Doxil (PEGylated liposomal doxorubicin), Abraxane (paclitaxel-anchored albumin), Marqibo (liposomal vincristine), DepoCyt (liposomal cytarabine), Oncaspar (PEG-asparaginase), and Genexol-PM (polymeric micellar nanoparticles [NPs]).^[4–7] Some delivery systems also demonstrated effective drug transportation abilities and controlled release features, which allowed them to release their cargo without any delay in reaction, in response to an external physical stimulus (such as sound, light, and magnetic field).^[8–11] Despite recent advances in responsive inorganic nanomedicine, drugs are often left tethered to or adsorbed onto the outer surfaces of particles (gold, graphene, carbon, iron oxide, or silica) with limited payloads, thus leading to insufficient therapeutic dosages at the targeted site and modest survival benefits.^[12] Furthermore, most of these responsive particles (such as gold, graphene, mesoporous silica, and carbon) have limited degradation properties that did not meet the needs of clinics.^[13]

1. Introduction

Hierarchical nanosized drug delivery systems (DDSs) offer versatile strategies for promoting the abilities of existing

Dr. B. Nirosha Yalamandala, Dr. W.-T. Shen, Dr. S.-H. Min, Prof. S.-H. Hu
Department of Biomedical Engineering and Environmental Sciences
National Tsing Hua University
Hsinchu 300, Taiwan
E-mail: shhu@mx.nthu.edu.tw

 The ORCID identification number(s) for the author(s) of this article can be found under <https://doi.org/10.1002/anbr.202100014>.

© 2021 The Authors. Advanced NanoBiomed Research published by Wiley-VCH GmbH. This is an open access article under the terms of the Creative Commons Attribution License, which permits use, distribution and reproduction in any medium, provided the original work is properly cited.

DOI: 10.1002/anbr.202100014

Prof. W.-H. Chiang
Department of Chemical Engineering
National Chung Hsing University
Taichung 402, Taiwan

Dr. S.-J. Chang
Department of Obstetrics and Gynecology
Hsinchu MacKay Memorial Hospital
Hsinchu 300, Taiwan

Therefore, resolving these obstacles will have an obvious impact on tumor treatment and patient wellbeing.

The synthesis of nanomaterials can alter the versatile functions of materials for various scales. With the integration of inorganic and organic chemistries in a single material, metal-organic frameworks (MOFs) provide not only molecular-structural control, tunable porosity, and chemical functionality but also sophisticated inner and outer surface features.^[14] MOFs were first reported in 1989 and were derived as coordination networks with potential porosity (guest adsorption on a crystal phase).^[15–17] In the 1990s, MOFs were prepared as task-specific materials by exploiting functional group variety to tune their size and geometry.^[18,19] These inorganic–organic crystalline frameworks are made by a process known as reticular synthesis, which can be easily modulated using the extended network structures of metal nodes and organic linkers.^[20,21] Furthermore, the choice of MOF constituents can give extremely high porosity (free volume up to 90%), and the functions of MOFs may be manipulated by chemical constituents placed along or within the backbone.^[22–25] The synthetic processes of MOFs have been widely developed through multiple strategies, such as diffusion, hydrothermal (solvothermal), electrochemical, and microwave processes. In contrast, postsynthetic modifications of MOFs are useful for further introduction of functionalities.^[26,27]

Industrial applications of MOFs, which include applications in catalysis, nonlinear optics, gas storage (employing highly porous MOFs), and separations, have increased the number of possible biomedical applications.^[28–31] For tumor therapy, nanoscale MOFs exhibiting passive targeting have received a great deal of attention in drug delivery systems (DDSs) due to their specific intrinsic and extrinsic properties. For example, not only are high porosity and surface area advantageous for improving drug loading efficiency, but characteristics such as good tenability, good biocompatibility, solubility in water, and biodegradability can also enhance bioavailability.^[32] Therefore, among stimuli-responsive materials, MOF-based systems have gained considerable interest for attaining controllable drug release.

The mechanism of action for MOFs in stimuli-responsive DDSs can be manipulated with the design of the organic and inorganic components. For example, coordination bonds of MOFs are highly sensitive to the external pH. Under weakly acidic conditions (similar to those of tumor microenvironments) this induces protonation to break coordination bonds, facilitating release of encapsulated drugs. The release of metal ions can further induce the Fenton reaction or elicit immune responses.^[33] Furthermore, the stability of the host–guest system in MOFs is weak due to the increased entropy of molecular recognition, leading to faster drug release while increasing the temperature. With the coordination of magnetic molecules or loading of magnetic particles, these systems can also exhibit magneto-responsive properties in targeted tumors. Generally, these triggers are classified as extrinsic or intrinsic. This review summarizes various MOF-based stimuli-responsive systems, including those displaying a single stimulus or multiple stimuli (**Figure 1**), which enable the controlled release of therapeutic agents upon triggering by exogenous stimuli such as light, temperature, magnetic field, enzymes, or endogenous stimuli, including ATP, pH, and redox stimuli (**Table 1**). The physicochemical properties of MOFs and pharmacological strategies for improving their responsiveness

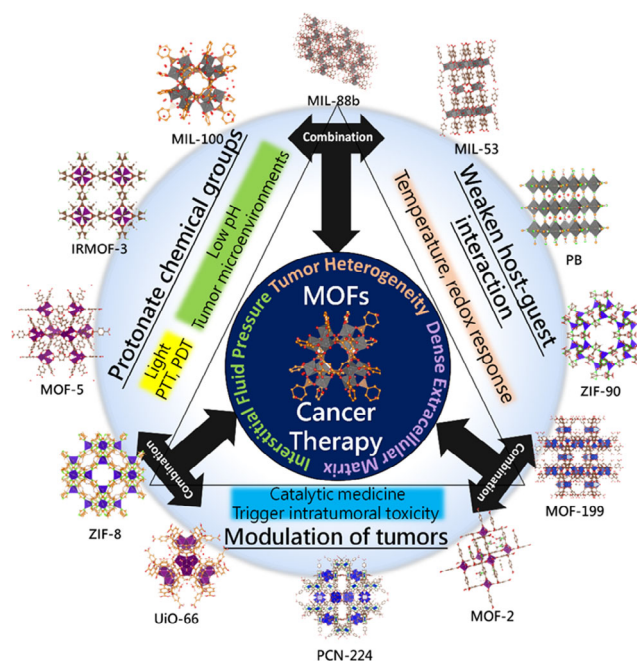


Figure 1. Scheme of different MOF strategies for on-demand drug release developed in recent years. MOFs exhibiting various physically or chemically responsive properties achieve precise on-demand drug release and energy generation (thermal or dynamic therapy).

are also described. Based on the responsiveness, catalytic therapies (induced by the Fenton reaction of MOFs) involving the utilization of existing high levels of H_2O_2 in cancer cells and the delivery of large antigen payloads constitute a new strategy for enhancing tumor therapies that potentially elicit immune responses. In contrast, the issues impeding clinical translation are also discussed, including overcoming tumor heterogeneity, recognizing the innate immune system and overcoming side effects. It is believed that this review can help scientists understand the progress, current excitement, potential issues, and clinical limitations of MOF DDSs for cancer therapy.

2. Single Stimulus MOFs

2.1. pH-Responsive MOFs

Compared with normal tissue, extracellular tumor tissue exhibits a slightly lower pH due to abnormal cell growth, which rapidly consumes nutrients and induces CO_2 generation, thereby decreasing the local pH (6.5–6.7) of the tumor microenvironment. Via passive targeting (known as the effect of enhancing permeation and retention [EPR effect]), nanosized MOFs could be accumulated at the tumor site. Environmental pH changes can actuate dissociation, disassembly, size transition, or even tuning of surface charges and morphologies, which are beneficial for controlling drug release from MOFs.

During the formation of MOFs, reactions run under acidic/basic conditions play a critical role in influencing the crystallization, coordination and growth of MOF hybrids.^[34,35] The coordination bonds of MOFs are highly sensitive to the external

Table 1. Integration of functional MOF with pH, temperature, magnetic field, light, enzyme, and multiple responsive strategies for drug delivery for tumor therapy.

Stimuli	MOF composite	Functionality	Therapeutic remarks	Refs.
pH	MOF(Fe)-GOX	Chemo, PDT	CPT delivery for HeLa cells	[48]
	PPY@MIL-100	PTT, Chemo	DOX delivery for HeLa cells	[43]
	DMH NPs	Chemo, PDT	DOX delivery for MCF-7 cells	[44]
	AuNCs@MOF	PDT, Chemo	DOX delivery for 4T1 cells	[52]
	ZIF-8	Catalysis, Bioimaging	DOX delivery for MCF-7 cells	[53]
	UMOFs@D@5	UCL, MRI	DOX and 5-Fu delivery for HeLa cells	[49]
	IRMOF-3@Gel	Chemo	DOX and Celecoxib delivery for SCC-9 cells	[79]
	Fe304@MIL	Drug delivery	Celecoxib delivery for NIH-3T3 cells	[45]
	Antigen/Eu-MOF	Immune responses	Antigen delivery for RAW264.7 cells	[55]
	ZIF-NAN	Intracellular cargo release	CPT delivery for HeLa cells	[51]
	pd@MOF-3	pH responsive	–	[54]
	MIL-101	Drug delivery	DOX delivery for MCF-7 cells	[59]
	Uio-66-N	Enhanced cellular uptake	DOX delivery for HeLa cells	[93]
	MIL-100	Biodegradability	–	[64]
	Zr-MOF	Proton conduction	–	[61]
	MIL-125-NH2	Colloidal stability	HeLa cells	[63]
	Temperature	Zr-based MOF	Thermal sensitive	Heating-activated drug release
MOF- derived PNIPAM		LCST phase transition	Drug release at high temperature	[71]
MIL-101(Cr)		Water capture	Calcein delivery for HeLa cells	[80]
MIL-100		Catalytic activity	–	[91]
MIP-200		Water sorption	–	[85]
MIL-53		Drug delivery	Ibuprofen	[156]
MIL-53-NH2		Gas sorption	–	[157]
MIL-100		Drug delivery	Genistein delivery for MCF-7 cells	[46]
MIL-100		Cosmetic patches	Cutaneous devices	[47]
Light		Ce6@RMOF	PDT	4T1 tumors
	ZIF-8	Catalytic activity	–	[102]
	MFC-N-100	Dye removal	Adsorption capacity for methylene blue	[96]
	Azo-Uio-66	CO2 separation	–	[101]
	NaGdF4:Yb	PTT, CDT	CT26 tumors	[121]
	MOF Cu (II)	PDT	CPT delivery for 4T1 tumors	[109]
	MnFe204@PEG	PDT	HeLa cells	[116]
	Mn304-PEG	PDT	4T1, HeLa, HUVEC cells	[117]
	ZIF-8	PDT	HepG2 cells	[118]
	HA	PDT	DOX for HEK 293 T cells	[125]
	MIL	Photoswitchable properties	Heat treatment	[123]
	MIL	Catalytic effect	–	[124]
	Enzyme	Pd-MOF	PTT, PDT	DOX delivery for HeLa cells
Mn-SS@PDDA		Redox-sensitive	DOX delivery for HeLa cells	[129]
CCM@MOF-Zr(DTBA)		Redox-sensitive	–	[130]
Mn(III)		PDT	–	[134]
HA-PCN		Chemo and PDT	–	[142]
ATP/pH	ZIF-90	Drug delivery	DOX delivery for MDA-MB-231 cells	[160]
Dual pH	MHzNs	Drug delivery	DOX delivery for SMMC-7721 cells	[77]
enzyme/pH	ZIF-8	PTT and FI	ICG delivery for SMMC-7721 cells	[126]
pH/Temp	MIL-101(Fe)	Chemo, PDT	DHA delivery for HeLa cells	[127]

Table 1. Continued.

Stimuli	MOF composite	Functionality	Therapeutic remarks	Refs.
pH/Redox	MIL-68	Redox activity	Lithium battery capacity	[147]
pH/Redox	UiO-66.NH2	Controlled drug release	5-Fu delivery for MDA-MB-231 cells	[131]
pH/Redox	ZIF-8	pH and redox responsive	DOX delivery for MDA-MB-231 cells	[158]

pH.^[36–38] Furthermore, the coordinative interaction of oligohistidine-tags (His-tags) with MOF NPs can anchor various molecular units, and then, released then in the acid medium of cancer cells.^[39] To achieve a pH-responsive MOF, the key strategy is to induce intrinsic protonation to break the coordination bonds. Normally, MOFs are constructed from metal ions and organic ligands, in which the organic ligand is composed of chemical groups such as imidazole, carboxylate, or pyridyl. When exposed to low pH, these deprotonated chemical groups are protonated, resulting in the loss of coordination bonds between the metal and ligand and leading to destruction of the MOF and delivery of encapsulated drugs in the tumor region.^[40–42] For example, an iron-based MOF (MIL-100) served as a shell composed of ferrous ions, and 1,1'-(1,4-butanediyl)bis(imidazole) (bbi) was coated on polypyrrole (ppy) NPs. MIL-100 exhibited a large surface area for encapsulating doxorubicin (DOX) when it was introduced into a solution of the ligand (Figure 2).^[43] When coated with a MIL-100 shell, DOX could be loaded effectively and showed pH-controlled drug release. At pH 5.0, more than 80% of the encapsulated DOX was released from MIL-100, a process attributed to the gradual degradation of the MIL-100 structure in an acidic environment. Furthermore, the amine groups on the DOX molecules also caused DOX to develop positive charges in acidic environments,

thereby weakening the electrostatic interactions between DOX and the MIL-100 shell. The loss of binding triggered the pH-responsive drug-release of DOX-loaded MIL-100. DOX release in endocytosis and enhancement of cancer cell destruction improved the cancer cell suppression.

Another MOF with DOX-loaded MIL-100 and hyaluronic acid (HA) coated on the surface of the NPs has been reported.^[44] The advantages of these NPs were as follows: first, the nanocarrier-loaded DOX efficiently, and through the Fenton reaction, hydroxyl radicals were generated for chemodynamic therapy by MIL-100 in the presence of H₂O₂. HA was coated on the MIL-100 surface to improve the dispersibility of MIL-100 and targeted MIL-100 toward tumor tissues. Thus, these NPs reduced drug toxicity and enhanced the efficacy of antitumor therapy through the combination of chemotherapy and chemodynamic therapy.

Lajevardi et al. reported magnetic and highly porous nano-carrier MIL-100 (Fe)@Fe₃O₄@SiO₂ NPs for delivery of celecoxib (a hydrophobic model drug) into target tumor cells.^[45] The release and loading efficiency of celecoxib in this system were investigated under different conditions. The results showed that the drug was released under acidic conditions (pH 3), and the adsorption capacity was high at physiological pH (7.4).

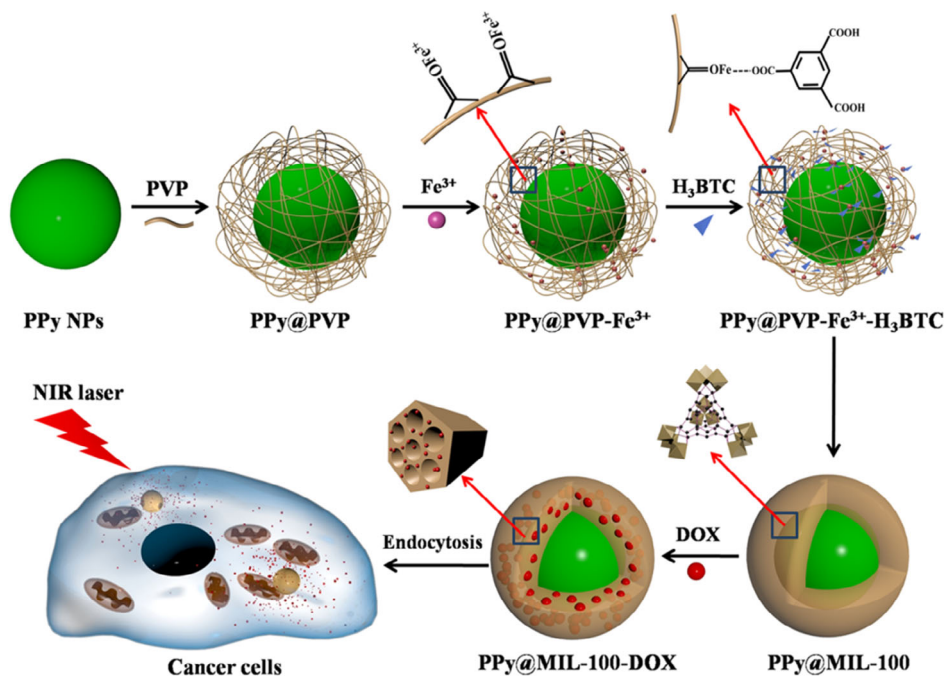


Figure 2. Schematic presentation of porous MIL-100-coated PPy particles for cancer therapy. MIL-100 was loaded with DOX and exhibited pH-controlled drug release at lysosomes via dissociation of the binding mechanism. Reproduced with permission.^[43] Copyright 2016, American Chemical Society.

Furthermore, the NPs had good biocompatibility with normal cells and exhibited controlled drug release under acidic conditions inside the cancer cell. Based on this unique feature of MIL-100(Fe), another study reported the use of mesoporous MIL-100(Fe) encapsulating a large payload of hydrophobic antioxidant and antiangiogenic molecules (bioflavonoid genistein [GEN]) and improving genistein oral bioavailability.^[46] GEN delivery studies were estimated with simulated physiological conditions and exhibited sustained release for 3 days. High bioavailability was also observed with the oral administration of GEN-loaded MIL-100 in a mouse model. Moreover, MIL-100(Fe) and biopolymers were used to develop cutaneous patches for the skin, and high caffeine loading was detected in cutaneous devices with progressive release.^[47] Such MOF-based cosmetic composites display potential in cosmetic applications.

An intrinsic pH-responsive MOF to enhance intracellular drug release was also applied with an Fe-based MOF (Fe-MOF) loaded with the drug camptothecin (CPT); this MOF used a cascade reaction involving the modified enzyme glucose oxidase on the MOF (Fe) surface.^[48] In acidic cell endocytosis, starvation therapy was enabled by choking off the supply of glucose as endogenous glucose was converted into H₂O₂ and H⁺ in a process catalyzed by GOx. An acidic tumor microenvironment was then generated, and H⁺ brought about MOF(Fe) degradation that resulted in the release of CPT and Fe³⁺. Finally, the generation of H₂O₂ was catalyzed by Fe³⁺ in OH-enabled reactive oxygen species (ROS)-mediated therapy. Combination therapy exhibited glucose transporter overexpression to kill cancer cells in an acidic environment in the tumor microenvironment, which provides advantages both *in vitro* and *in vivo*. In addition, Ling et al. reported a MOF loaded with two drugs (DOX and 5-fluorouracil [5-FU]) for tumor therapy.^[49] This pH-responsive nanosystem also displayed effective drug release and MOF disruption under acidic conditions. In comparison with systems loaded with one kind of anticancer drug, the dual drug nanosystem showed great cytotoxicity. The two drugs released from the nanosystem exhibited cooperative effects. The HeLa cells used in this study showed high cellular uptake efficiency. By coating it with a NaGdF₄ shell, the MOF also demonstrated efficacy in T₁-weighted magnetic resonance imaging.

zeolitic imidazolate framework (ZIF), a Zn-based MOF system, was also widely used in a pH-responsive DDS MOF with protonated chemicals. ZIF-8 is a pH-responsive DDS MOF with a combination of Zn²⁺ and 2-methylimidazole and large pores and drug loading capacity; it is highly acid sensitive and has been heavily investigated.^[50] Modifying the synthesis of ZIF and encapsulating DOX in ZIF-8 through a single pot process resulted in a 20% loading of DOX in ZIF-8. After 7 days, the nanosystem showed stability without releasing DOX at 60 °C in a PBS solution (pH 7.4), whereas ≈90% of the DOX was released from the nanocarrier at pH 5.5 due to the decomposition of the nanocarrier structure in an acidic environment. According to the (3-(4,5-dimethylthiazol-2-yl)-2,5-diphenyltetrazolium bromide) (MTT) assay, the nanosystem exhibited high efficacy toward breast cancer cell lines. Another example was reported by Tolentino et al., in which ZIF-8 was loaded with surfactant deoxyribonucleic acid (DNA) as a nucleic acid nanocapsule (NAN).^[51] The results illustrated great nanocarriers that could be accommodated in the formation of NANs, and the

stability of the MOF under biological conditions was simultaneously improved. The control of the outer shell of the NAN provided a high degree of control over the accessibility of the MOF environment, requiring particular enzymes present in acidic conditions to release the encapsulated cargo. This results in a double-gating mechanism providing a high degree of control with two enzyme activities and MOF cellular delivery assays.

To improve the cancer therapeutic effects, the subsequent combination of pH-responsive drug release and external physical treatments was used. For example, Zhang et al. synthesized a nanocomposite with DOX loaded in ZIF-8-coated gold nanoclusters (AuNCs@MOF-DOX).^[52] The nanoprobe showed great effectiveness in chemotherapy and photodynamic (PDT) therapy under acidic conditions, where the ZIF-8 structure collapsed and exhibited accelerated DOX release. In addition, the synergistic effect of chemo/PDT therapy was achieved by the separation of AuNCs from AuNCs@MOF-DOX. After treatment with the nanoprobe *in vivo*, the 4T1 tumor (mammary carcinoma) was inhibited completely by the combined chemo/PDT therapy, indicating the importance of AuNCs@MOF-DOX as a bifunctional pH-responsive nanoprobe for efficient chemo/PDT in the treatment of breast cancer. Furthermore, the multifunctional pH-responsive MOF (ZIF-8/DOX-PD-FA) integrated with Si-Gd NPs combined the photosensitizers (PSs) chlorine e6 (Ce6), DOX, ZIF-8, and folic acid–poly(ethylene glycol) (PEG-FA) in one platform.^[53] This pH-sensitive MOF realized the release of DOX through swelling in an acidic tumor microenvironment. The cytotoxicity results showed that nanocarriers plus near-infrared (NIR) radiation caused a higher level of MCF-7 tumor cell death compared with other nanocarriers. As expected, the nanocarriers accumulated successfully at tumor sites, as displayed by both magnetic resonance biomedical imaging and fluorescence.

Jiang et al. reported another MOF, UiO-66, a pH-responsive nano metal–organic framework (NMOF) that is readily prepared with an uncomplicated lab synthesis and is composed of a zirconium oxide complexes bridged by terephthalic acid ligands.^[54] This NMOF had great stability and is highly effective in numerous applications. The thermodynamic stability of UiO-66, which is caused by the strong Zr–O bond, has provoked excitement; in fact, without the coordination bond, the carbon–carbon bonds in the ligand break. The authors demonstrated that poly[2-(diethylamino)ethyl methacrylate] was transplanted onto UiO-66 NPs through a postsynthetic approach for the generation of PDEAEMA-g-UiO-66. Pd NP-encapsulated PDEAEMA-g-UiO-66 was synthesized by solution impregnation. Furthermore, it displayed pH-induced emulsifying and demulsifying behaviors induced by alternate protonation–deprotonation of the amino groups of PDEAEMA. This Pickering emulsion system could be recycled at least five times without loss of its catalytic activity, and it is robust.

Through breakage of the coordination bonds between metal and ligand, the destruction of MOFs in other systems was also applied in the local delivery of encapsulated drugs. Duan and co-workers reported a MOF self-assembled by Eu³⁺ ions and guanosine monophosphate and loaded with an antigen for cancer therapy (Figure 3). The method gave high loading capacity and the efficiency of the antigen release was ≈55 wt%; moreover, the MOF-loaded antigen displayed pH-dependent drug delivery behavior. In addition, a pH-responsive codelivery system enhanced antitumor outcomes.^[55] Antigen was released over 48 h at pH 7.4, whereas 60% of the antigen

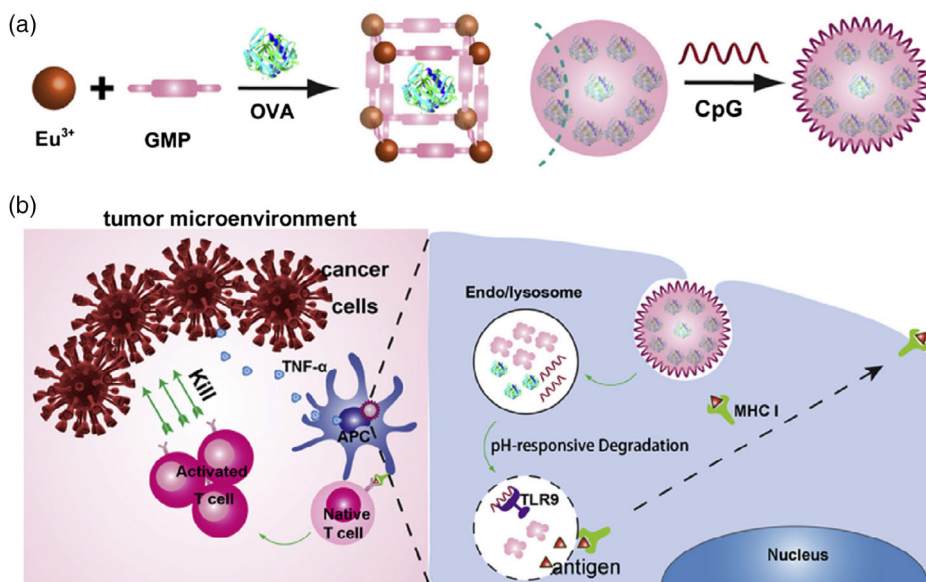


Figure 3. Schematic presentation of a pH-responsive and antigen-loaded MOF. Upon uptake by immune cells, the lanthanide ion- and guanine mono-phosphate-coordinated MOFs degraded at the endo/lysosome to release the loaded antigens and CpG. Reproduced with permission.^[55] Copyright 2017, Elsevier Ltd.

was released at pH 5.0, because of the dissociation of MOFs in the acidic environment. The authors indicated that codelivery of antigens and immunostimulatory molecules was very easy, suitable, and effective, showing no toxicity in vivo or in vitro. Furthermore, to effectively suppress lung tumors, Simon-Yarza et al. reported a biodegradable mesoporous iron(III) polycarboxylate MOF with pH-responsive and reversible aggregating behavior designed to target the lung for drug delivery (Figure 4).^[56] The particles spontaneously aggregated in the lung capillaries and then disaggregated within 24 h, facilitating the release of the encapsulated drug in a lung metastasis model.

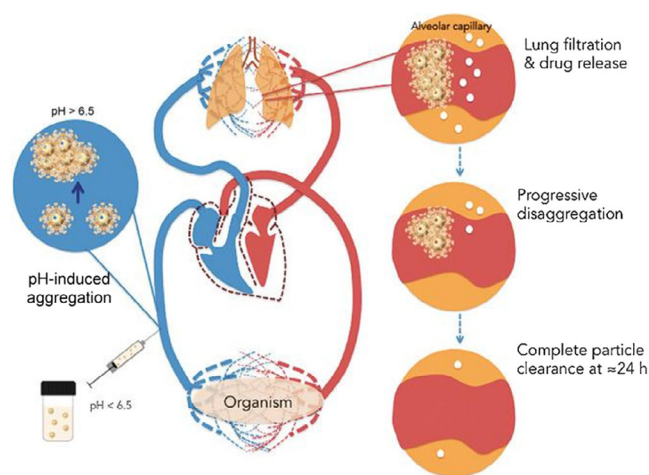


Figure 4. A biodegradable iron-based MOF with pH-responsive and reversible aggregating behavior was developed to target the lung. The particles were able to spontaneously aggregate at the lung capillaries and disaggregate within 24 h. Reproduced with permission.^[56] Copyright 2017, Wiley-VCH Verlag GmbH & Co. KGaA, Weinheim.

Jin et al. reported a theranostic MOF-based DDS for the treatment of bacterial endophthalmitis that posed a serious threat to humans.^[57] The lipopolysaccharide-modified UiO-66-NH₂ MOF was loaded with toluidine blue (TB, used as a PS) to enhance the efficiency of PDT. Via a unique pH-responsive feature, TB was released at pH 5.5. Both in vitro and in vivo antibacterial tests demonstrated that the as-synthesized MOFs exhibited outstanding antibiofilm properties due to ROS generation upon irradiation.

Another MOF design was reported by Chen et al. for the treatment of endophthalmitis.^[58] In this study, a bacterial infection was treated with a pH-responsive zeolitic imidazolate framework-8-polyacrylic acid (ZIF-8-PAA) developed for infection-targeted delivery of ammonium methylbenzene blue (MB) via in situ reduction of AgNO₃/dopamine to silver NPs. The particles demonstrated targeting and antibacterial properties through the combination of Ag/PDT, facilitating antibacterial activity toward *E. coli*, *S. aureus*, and methicillin. Both in vitro and in vivo studies revealed the excellent biocompatibility and antibacterial function of these composite nanomaterials.

Responsive MOFs have also been used for the targeted intracellular delivery of therapeutic agents. Using real-time cell analysis, Markopoulou et al. identified intracellular cargo release mechanisms differing from those of MOFs in vitro.^[59] With extracellular acidification, lipid-coated MIL-100 containing iron and trimesic acid was reported to produce iron ions via the degradation of the MOF composites, leading to cancer cell death.^[60] With a different design, zirconium MOF MIP-202 (Zr) prepared with natural α -natural amino acids displayed proton conduction features, excellent chemical stability, and a wide pH range.^[61] After modifying the linker molecules with intrinsic fluorophors, the Zr-based MOF demonstrated various photoluminescence properties.^[62] In addition, the nanometric

MIL-125-NH₂ MOF was applied as a potential carrier of a nerve agent antidote, in which the nerve antidote was encapsulated into MOF pores through π -stacking and hydrogen-bonding interactions.^[63,64] The as-synthesized MOF exhibited good colloidal stability and has potential for biomedical applications. Remarkably, the release of guest molecules was predicted and programmed by precise MOF design with multiple functional groups for the control of guest release profiles.^[65] Despite pH-responsive MOFs have many advantages, there are still some critical issues for tumor therapy: 1) Although the tumor tissue has a local pH (6.5–6.7) lower than that of the microenvironment, the difference in acidity might be too minor to efficiently trigger the pH responses of the MOF. 2) The dissociation or disassembly of MOFs can lead to toxicity due to the release of metal ions in healthy organs. 3) The pH-triggered aggregation of MOFs sometimes causes weak tumor penetration ability.

2.2. Temperature-Responsive MOFs

Temperature-responsive DDSs have been widely developed with both organic and inorganic materials. If the drug has suitable molecular size and characteristics, the porous MOF can adsorb it on pore surfaces via physical adsorption.^[66] However, host–guest interactions using secondary bonds, including π – π interactions, dipoles, charges, or hydrogen bonds, are not as strong as chemical bonds. Upon heating, the stability of the host–guest interactions is lost due to the entropy cost characterizing the molecular recognition. Therefore, fast release rates can be triggered by weakening host–guest interactions at high temperatures.^[67–69] In this regard, a Zr-based MOF- (ZJU-801, Zhejiang University) released encapsulated drug molecules by breaking the π – π interactions between drug molecules and the MOF when the temperature was raised.^[70] The release rate was 10-fold greater at 60 °C than at 25 °C. The main mechanism involved the decreased π – π interactions between the MOF and drug molecules, resulting in an on-demand release.

Another strategy for using the temperature responses of MOFs is to modify their porous surface with thermo-responsive polymers, e.g., poly(*N*-isopropyl acrylamide) (PNIPAM), which possesses a reversible lower critical solution temperature (LCST) phase transition from a hydroswollen state to a shrunken dehydrated state.^[71–76] In other words, this polymer is hydrophilic and dissolves in water when the temperature is below the T_c at ≈ 32 °C, yet it also forms aggregates.^[77–79] Using this unique feature, Karmakar et al. (Figure 5) reported that a chromium-based MOF (MIL-101) modified by PNIPAM exhibited thermo-responsive water capture and release behavior.^[80] Forty percent water content could be captured by a MOF at 96% RH and 25 °C. Water capture was $\approx 98\%$ and, importantly, it could be realized under mild conditions because of the hydrophilic/hydrophobic transitions of the PNIPAM component. Furthermore, smart PNIPAM-modified UiO-66 loaded with resorufin, caffeine, and procainamide by immersion exhibited temperature-responsive drug release at the transition temperature, exemplifying controlled release driven by temperature changes.^[81,82] However, temperature control is a critical problem

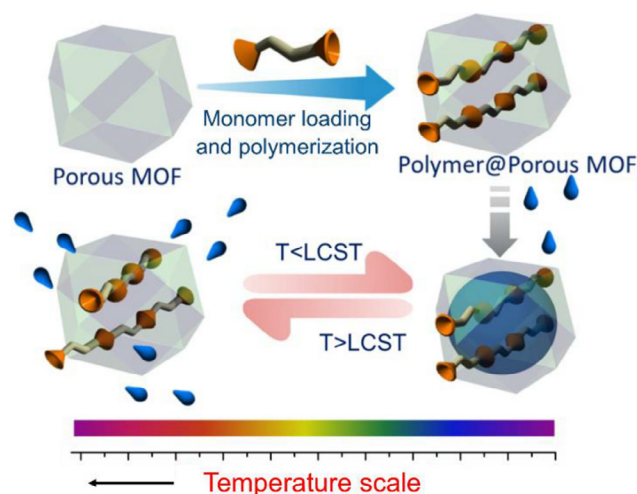


Figure 5. Thermo-responsive polymer (poly(*N*-isopropyl acrylamide) (PNIPAM)-modified MOFs exhibit a reversible lower critical solution temperature (LCST) phase transition from a hydroswollen state to a shrunken dehydration state. Reproduced with permission.^[80] Copyright 2020, Wiley-VCH.

around tissues, and the increase temperature might also induce side effects.

The synthesis of MOFs at room temperature is of specific interest and is a prerequisite for the incorporation of biomolecules in biomedical applications. Most recently, Dai et al. (Figure 6) reported a one-step, room temperature synthesis of highly porous metal(IV) carboxylate MOF systems containing five 12-connected and two 8-connected M_6 oxo-clusters with different functionalized organic ligands.^[83] Furthermore, scale-up of the synthesis involved the use of a 5 L pilot-scale system, giving evidence of a high yield for room temperature syntheses of Zr-based MOFs.

The stability of MOFs is another important issue in biomedical applications. Recently, an ultrastable titanium-carboxylate MOF^[84] and MOFs with hydrolytic stability^[85,86] were developed for potential applications. Furthermore, ionothermal synthesis offered a new approach for MOF preparation.^[87,88] The unique functions of MOFs can be used for gas delivery and catalytic reactions, facilitating further modulation of the tumor microenvironment.^[89–91] In contrast, in gene therapy, both MIL-100 and UiO-66 have been reported to maintain the complete sequence of nucleic acids for delivery into the cytoplasm.^[92,93] Moreover, enhanced gene expression and cell death were displayed by a mitochondria-targeted MOF system.^[94]

2.3. Magnetically Responsive MOFs

By incorporating magnetic materials, magnetic MOFs can exhibit magnetic targeting ability and serve as a contrast agent for magnetic resonance imaging (MRI).^[95,96] In addition, an alternating magnetic field (AMF) was able to remotely actuate magneto-hyperthermia effects for tumor treatments in which the temperature can increase to more than 43 °C; this is mainly attributed to the dissipation of magnetic energy (Brown and Néel

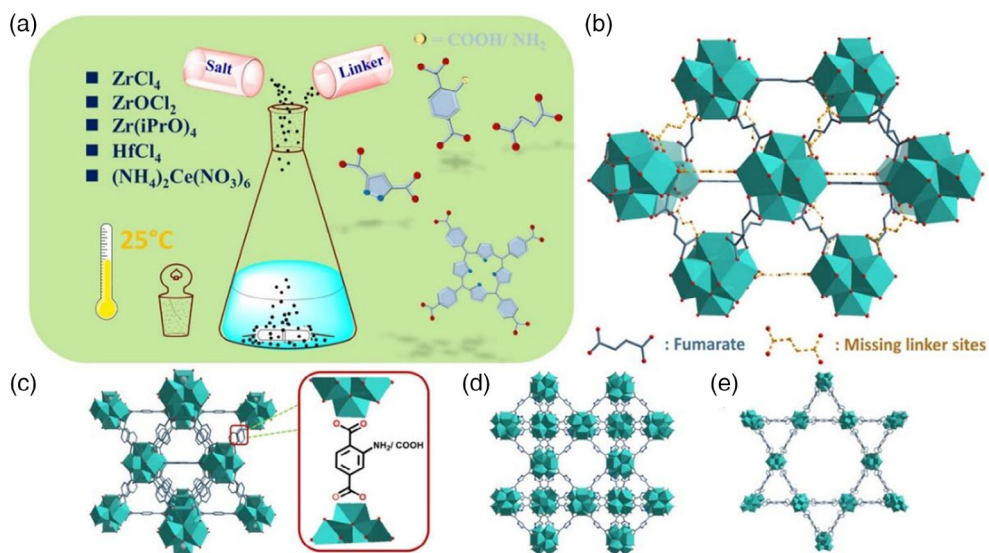


Figure 6. Schematic presentation of porous metal (IV) carboxylate MOFs (Zr, Hf, Ce) containing 8- or 12-connected micro-/mesoporous solids with different functionalized organic ligands. Reproduced with permission.^[83] Copyright 2021, Wiley-VCH.

relaxation) that is detrimental to crystals, among other factors.^[53] Based on this magnetothermal effect, a MOF-derived $\text{Fe}_3\text{O}_4@\text{C}$ composite integrated with hyperthermia and chemotherapy functions triggered by magnetic fields was reported (Figure 7).^[97] With DOX loading, the NPs showed high magnetic heating efficiency and magnetic field-triggered on-demand release capability. Using these synergistic effects, the NPs efficiently suppressed tumor growth in vivo. The large proportion of cell apoptosis and necrosis at the tumor were responsible for the inhibition of the tumor. However, AMF might work on the main clearance organ, where a large portion of the magnetic MOF usually accumulates, potentially inducing severe side effects. Therefore, methods for focusing the AMF on tumors is of critical importance.

In MOFs, decorated magnetic materials served as magnetically guided targeting and T_2 contrast agents for magnetic resonance imaging. When combined with the necessary expertise, the magnetically responsive MOF is a promising material for drug delivery and cancer therapy. Magnetically responsive MOFs reveal unique properties in drug delivery because of major advantages in magnetic targeting, magnetic separation, and magnetic resonance imaging. Magnetically guided anticancer drug delivery is a great way to develop therapeutic efficacy by loading drug therapeutic probes in tumor regions.^[98,99] In this regard, newly developed strategies incorporated magnetic NPs to address separation and MOF handling. The magnetic properties of MOFs have been a receiving interest due to the integration of both magnetic properties and various MOF features into one

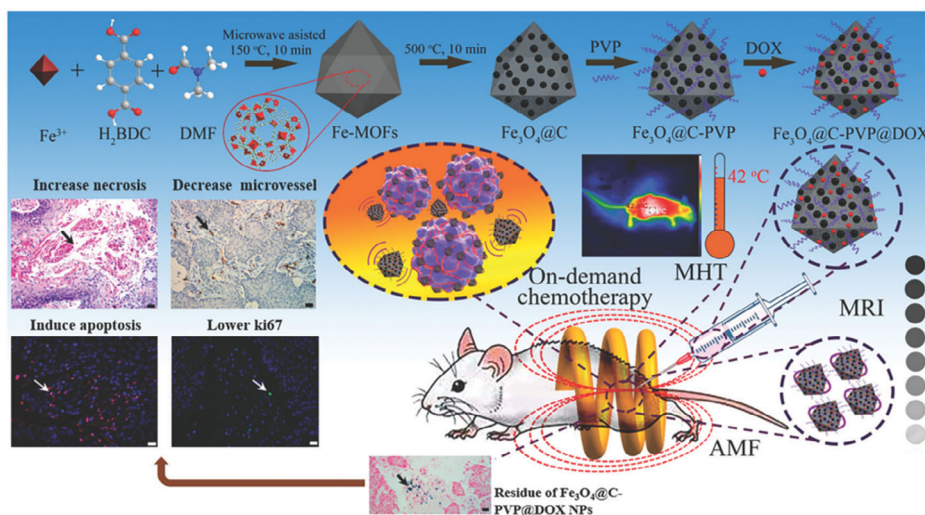


Figure 7. Through the magnetothermal effect, a magnetic field-responsive MOF-derived $\text{Fe}_3\text{O}_4@\text{C}$ composite integrated magnetic-triggered hyperthermia and chemotherapy functions. Reproduced with permission.^[97] Copyright 2013, Royal Society of Chemistry.

material.^[100–102] For example, an Fe₃O₄-decorated MOF loaded with nimesulide (a drug) exhibited magnetic resonance imaging and controlled drug release for treatment of pancreatic cancer.^[60] In contrast, another magnetically responsive MOF-based delivery composite for magnetic targeting and nuclear magnetic imaging was also developed for both in vitro and in vivo cancer therapy.^[61] With the guidance of an external magnetic field, particle accumulation and therapeutic effects were significantly improved. Through this magnetic-guided targeting, the MOF demonstrated effective drug delivery to the targeted site and suppressed tumors.^[103,104] In addition to iron oxide, another common positive contrast agent, gadolinium (Gd³⁺), was also applied to a MOF via molecular chelation, which not only stabilized Gd³⁺ but also reduced its toxicity. For example, Xue and colleagues reported a reversible addition-fragmentation chain transfer (RAFT) copolymer-modified Gd³⁺ MOF used to decrease the side effects of Gd³⁺ for MRI.^[105]

2.4. Photo-Responsive MOFs

In the past decade, photo-responsive (or light-responsive) materials for tumor therapy have received great attention because they exhibit minimally invasive and effective photoablation of targeted tumors. Recently, many types of materials with strong light absorptivities have been used in photothermal (PTT), PDT, and photoacoustic (PA) treatments for killing cells, including gold, graphene, carbon-based materials, CuS, and organic (chromophore) molecules.^[106,107] The requirements for PDT treatment include PSs, molecular oxygen, and light. These components generate reactive molecular species to target cells and induce apoptosis. This advances theranostic applications with active PSs. The release of PS molecules at the targeted site further enhances the PDT effect.^[108] However, the penetration depth might be an obstacle for this strategy.

With the coordination of a specific metal, the light-absorbing MOF spontaneously accumulates at the targeted tumor site (EPR effect), where PDT can be used to enhance the cell-killing effects. Upon irradiation, the triplet state of the MOF is excited via a short-lifetime singlet state, facilitating energy transfer to surrounding oxygen molecules for the generation of ROS, including singlet oxygen, superoxide anion radicals, hydroxyl radicals, and hydrogen peroxide, to damage and suppress tumor cells.

Although traditional PS-based PDT can produce ROS in cells, an increase in ROS amounts would reduce the glutathione (GSH) level and decrease the PDT efficiency. To solve this problem, Zhang et al. synthesized a Cu-based MOF to reduce the GSH level by absorbing GSH in cancer cells. In this system, Cu (II) was the active center for PDT.^[109] Once the NPs were taken up by cancer cells, high levels of ROS were produced upon light irradiation, and intracellular GSH was decreased due to absorption on the MOF. These synergistic effects enhanced the effect of PDT. Another enhanced design of MOFs for PDT involved an O₂-loaded CuTz-based MOF that can simultaneously overcome tumor hypoxia and reduce GSH levels in tumors (Figure 8).^[110] In cancer cells, this CuTz-based MOF induced a Fenton-like reaction to generate ·OH and O₂ in the presence of H₂O₂ and NIR irradiation, suppressing the tumor in vivo.

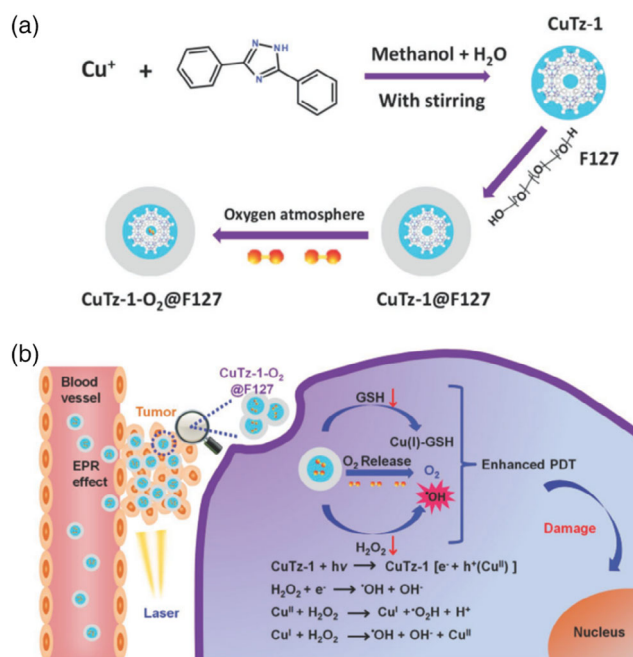


Figure 8. The O₂-loaded CuTz-based MOF simultaneously overcame tumor hypoxia and reduced GSH levels in tumors. In cancer cells, the MOF induced a Fenton-like reaction to generate ·OH and O₂ in the presence of H₂O₂ and NIR irradiation. Reproduced with permission.^[110] Copyright 2019, WILEY-VCH Verlag GmbH & Co. KGaA, Weinheim.

Xu et al. reported a ZnPc@ZIF-8 nanocomposite, which contained a water-insoluble PS (ZnPc) made via a coprecipitation method.^[111] To segregate and inhibit self-agglomeration and maintain ZnPc in a monomeric state, ZIF-8 microspores acted as molecular cages. In vitro studies revealed that the nanocomposite could be endocytosed by cancer cells and showed red fluorescent emission with great PDT for the treatment of cancer. However, the synthesized nanocomposite was sensitive to acid and degraded after PDT. This study has potential for solving the problems of PS bioavailability and solubility using MOFs as carriers. Finally, for efficient PS delivery, the nanocomposite ZnPc@ZIF-8 was developed, which has great luminescence intensity and highly efficient O₂ generation capability.

PTT for tumor or disease treatments was attributed to a light-absorbing agent when external electromagnetic radiation (usually with infrared wavelengths) was applied. The electrons were excited from the ground state to the excited state upon irradiation of the light absorber. Subsequently, energy relaxation through nonstable electron decay caused an increase in kinetic energy and heating of the microenvironments surrounding the light absorber.^[112,113] Therefore, light energy can be converted into heat or electrons to change material characteristics such as temperature, hydrophobicity, and chemical reactivity. For application of PTT, MOFs often improve the light-energy conversion through loading with a photo-responsive agent such as indocyanine green (ICG).^[114] For example, MIL-100 was loaded with ICG conjugated to HA to target CD44-overexpressing cancer cells. With the application of 808 nm irradiation, the PTT of the MOF suppressed cancer cells.

The incorporation of photoactive species into MOFs for use as photo-responsive agents is another strategy for fabricating light-activated MOFs. Several photoactive organic molecules exhibiting a wide range of interesting effects, including luminescence, energy harvesting, photon-upconversion, photoinduced conformational changes, and nonlinear optical properties, have been developed. To incorporate these molecules, the porosity of the MOF permits loading of chromophoric compounds as guests in the MOF pores.^[115–118] Simple operating techniques, time controllability, and zero energy costs have increased the attention given to light-triggered DDSs. Drug release controlled by conformational changes, PTT conversion or chemical cleavage under illumination is the major mechanism of photosensitive drug release. The design of ligands is also useful for the fabrication of photo-responsive MOFs incorporating particular photosensitive molecules as ligands.^[119,120]

For PTT using a MOF, Chen and co-workers reported a polypyrrole (PPy)-loaded MOF (PPy@MIL-100) made by reacting the iron ions on the surface with PPy during MOF growth.^[121] The nanocomposite showed strong absorption in the NIR and good PTT efficiency. Based on iron carboxylate materials, the structure of the MOF also possessed excellent capacity for the storage of DOX. DOX delivery was increased by the damage of the outer MOF core at low pH in the tumor microenvironment. When irradiated, heat generated from the nanocomposite resulted in the quick release of the encapsulated DOX from the MOF shell. The fabricated nanocomposite exhibited multiple modes of MRI, PAI, and chemo PTT therapy in vitro. This work demonstrated the design of multifunctional MOFs for cancer theranostics. A MOF useful for multimodal imaging and photo-immunotherapy was developed for PTT.^[122] The MOF served as a PA probe (by loading ICG), and immune adjuvants (cytosine-phosphate-guanine sequence, CpG) passively accumulated at the tumor site via the EPR effect and achieved PTT at the tumor site. Photoimmunotherapy was activated by PTT upon 808 nm laser irradiation, and then the tumor-associated antigen and CpG were released, facilitating the heating of cold tumors by activating the immune system (Figure 9). A similar strategy of loading a PS was also investigated by embedding photoswitchable spiropyran into a MOF for photoresponses.^[123] In addition, Dan-Hardi et al.

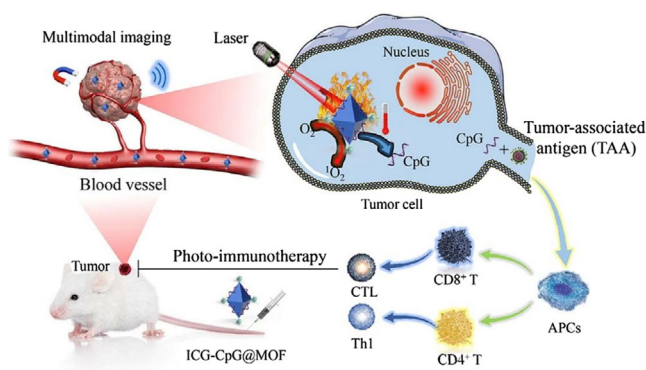


Figure 9. The functional MOF served as a PA probe (by loading ICG), and immune adjuvants (CpG) achieved PTT at the tumor site. Photoimmunotherapy was activated by PTT with 808 nm laser irradiation. Reproduced with permission.^[122] Copyright 2020, Elsevier Ltd.

reported a titanium-based MOF with oxo-hydro clusters and dicarboxylate linkers to induce reversible photochromic behavior. The composite has shown high photonic sensitivity, and the titanium oxo clusters were oxidized in the presence of oxygen and exhibited photocatalytic properties.^[124]

2.5. Redox-Responsive MOFs

The reducing environment of tumor cells is regulated mainly by the oxidation and reduction states of glutathione (GSH) and nicotinamide-adenine dinucleotide phosphate (NADPH), which possess great reducing capabilities. The concentration of GSH is greater than that of NADPH in a reducing environment, in which GSH plays an important role in tumor microenvironment regulation. GSH controls the cellular reducing environment via the fragmentation and formation of disulfide bonds. This is the reason why the GSH concentration is very important for a cellular reducing environment. The GSH concentration was higher in the intracellular tumor environment than in the extracellular environment. The GSH concentration in tumor tissues was 4 times higher than that in normal tissues. Based on these features, several DDSs have been designed for sensing the reducing environments of tumor tissues to trigger drug release by disulfide bond cleavage in GSH-sensitive materials.^[125,126] For example, in the reducing environment of tumor tissues induced by GSH, disulfide bonds can be utilized as linkers in DDSs to deliver cargoes by rapid degradation. The breaking of covalent bonds upon exposure to high GSH levels is the mechanism operating in this strategy. GSH causes faster depolymerization of disulfide bonds in a reducing environment than other redox carriers. In MOF systems, ligand design and surface modification are the main key uses for disulfide bonds.^[127,128]

In introducing the disulfide bond into the MOF ligand, Zhao et al. reported a GSH-responsive MOF system in which Mn-SS was fabricated with Mn^{2+} and dithiodiglycolic acid as ligands.^[129] For the successful release of the encapsulated drug (DOX), the cleavage of the disulfide linkage was carried out in the presence of GSH. Furthermore, the Mn^{2+} in Mn-SS@MOF also exhibited a stronger T_1 contrast in MRI for bioimaging. In addition, Lei et al. reported a redox-responsive MOF using zirconium (Zr), iron, and aluminum as metal nodes and the organic ligand 4,4'-dithiobisbenzoic acid (DTBA).^[130] Compared with normal tissues, the cleavage of the disulfide bonds in 4,4'-DTBA by GSH was obviously faster in tumor tissues. The composite also exhibited good size and other properties as a drug nanocarrier; it exhibited fast release of the drug when curcumin was encapsulated into the MOF, thereby enhancing tumor cell death. Furthermore, Liu et al. also constructed a redox-responsive and tumor-targeted MOF by anchoring functional disulfide anhydride and folic acid to the organic links of UiO-66- NH_2 MOFs.^[131] The overexpressed GSH in cancer cells attacked the thiolate moiety to cleave the disulfide bonds, leading to redox stimuli-responsive drug release in MOFs.

The drug release in redox-responsive MOFs in the tumor environment is mainly based on dissolution of redox-responsive chemicals. Common metal species, such as Cu(II) and MnO_2 , are redox active, facilitating GSH oxidation and degradation.^[132,133] Wan et al. prepared a MOF based on Mn(III) and

porphyrin (TCPP) via a single-pot method.^[134] Mn(III) not only quenched TCPP- fluorescence but also inhibited formation of ROS. These MOFs were decomposed by GSH into Mn(III) and free TCPP in the intracellular tumor region upon endocytosis by tumor cells; this resulted from the redox reaction between Mn(III) and GSH. TCPP release by regulation of GSH controllably implemented ROS generation under irradiation without adverse effects, including damage or inflammation, in normal tissues. Finally, with GSH unlocking, Mn(III)-sealed MOFs significantly improved the therapeutic efficacy of PDT by controlling ROS generation and depleting GSH after dual tumor homing.

The growth of glucose-responsive carriers has led to excellent research advances for treatment of diabetic patients. Glucose oxidase (GOx)-based insulin release is the most approved method for the glucose-responsive system. When the concentration of glucose is high in the cargos, GOx will convert glucose into gluconic acid and H₂O₂, which results in local acidification, facilitating insulin release by MOF degradation in an acidic environment. The MOF should be acid labile, as are MIL-100, ZIF-8, etc., to release the drug and achieve GOx/glucose responsiveness. The GOx/glucose-responsive MOF-based drug release system has a capacity for starvation of cells because of the consumption of glucose. In addition, it is used in a Fenton-like reaction in the enzymatic reaction.^[135] For example, Chen et al. reported a zeolitic Zn²⁺-imidazolate MOF (ZIF-8 NMOFs) for the glucose-responsive controlled release of drugs.^[136] ZIF-8 NMOFs loaded with glucose oxidase (GOx) and the GOx-mediated aerobic oxidation of glucose yielded gluconic acid and H₂O₂, leading to the degradation of the MOF and drug release. After treatment with glucose, the MOF was unlocked to release insulin. Furthermore, the degradation of MOFs also released the VEGF aptamer, which acts as a potential inhibitor of the angiogenic regeneration of blood vessels for the treatment of macular diseases in diabetic patients.

The use of enzyme-responsive MOFs has been identified as a unique method to successfully attain intracellular drug delivery. Several enzyme-responsive materials have been used, such as hyaluronidases, proteases, and pectinases. To deliver the anticancer drug to a specific site, these enzymes were degraded by special enzymes via redox reactions. The enzyme-responsive materials are the main consideration in enzyme-responsive mechanisms. The diffusion of these enzymes into MOF pores provides an approach to achieve high loading and low leaching of enzymes when utilizing mesoporous MOFs. Due to the complicated syntheses and harsh conditions, the degradation of the drug exhibits great potential applications.^[137–141] In this regard, Kim et al. reported an enzyme-responsive MOF composed of Zr-based porphyrinic MOFP (CN224 MOF) and HA.^[142] The MOF was coated by enzyme-responsive HA through multivalent coordination bonding between the Zr cluster and carboxylic acids of HA. The inherent properties of PCN-224 allowed PDT therapy in cancer cells. Furthermore, the encapsulated drug (DOX) could be introduced by the enzyme degradation of HA in cells.

To overcome the low therapeutic efficacy of chemotherapy, MOF-based catalytic medicine has been reported to generate high ROS levels at the intratumoral site in both endogenous and exogenous areas. In the past several years, MOF materials have been designed to trigger catalytic ROS generation at tumor sites for cancer therapy.^[143] Catalytic tumor starvation can also be realized by

intratumoral delivery of nanocatalytic agents for nutrient/oxygen depletions.^[144,145] However, the catalytic approach still suffers from a cell protective mechanism (known as autophagy) that mitigates ROS damage. To overcome this difficulty, the Shi and co-workers developed an iron-containing metal-organic framework [MOF(Fe)] nanocatalyst that served as a pharmacological autophagy inhibitor to augment ROS oxidation damage by generating a large amount of oxidizing ·OH radicals in cancer cells (Figure 10).^[146] Moreover, chloroquine was used to deacidify lysosomes and reduce autophagy, thus preventing cancer cells from extracting the inner components to detoxicate themselves.

In contrast, the redox properties of porous MOFs were applied in lithium-based batteries by Fateeva et al. They synthesized and characterized an Fe-based MOF (MIL-68) using hydrofluoric and hydrochloric acid under solvothermal conditions.^[147] MIL-68 acted as a good positive electrode for lithium-ion batteries.^[148] The MOF served as a semiconducting thin film and was also reported to revolutionize electronic and photonic devices.^[149]

3. Multistimuli-Responsive MOFs

To develop cancer therapies more precisely, multistimuli-responsive MOFs have been introduced. Because of the complications of the human body environment, developing efficacious DDSs usually requires multiple triggers rather than a single stimulus response.

3.1. Supramolecular Nanovalves/Gatekeepers on MOFs for Drug Controlled Release

Supramolecular nanovalves can serve as reversible linkages of multiple components for the transportation and release of drug molecules. Because of their unique features, functional supramolecules have been applied in several nanobased delivery systems to address the unwanted controllability and reduce side effects.^[150] For example, at low pH, the chemical bonds between these nanovalves and MOFs were potentially protonated to break the coordination bonds between metals and ligands, introducing encapsulated drug release at the targeted site. Tan et al. designed supramolecular monodisperse MOFs gated by a carboxylatopillar[5]arene with pH-triggered controlled drug release for degenerative diseases.^[151] This smart delivery system has shown large pore sizes for drug encapsulation and low cytotoxicity. Furthermore, the same group also applied the supramolecular valve in a controlled release system composed of Zr-MOFs and carboxylatopillar[5]arene. At various temperatures, the regulation of drug release by the gates was achieved. Moreover, Zn²⁺-triggered drug release has also shown potential advantages for brain disease therapy.^[152] Another supramolecular pseudorotaxane-capped Zr-MOF was developed for pH-responsive on-demand drug release for treatment of bone diseases.^[153]

Based on the functionality of supramolecular nanovalves, a pH/temperature dual-responsive pillar[6]arene-valved nano-platform for chemo-PTT therapy was also developed.^[154] Using layer-by-layer assembly and surface modification, the various modular components serving as cores were coated with UiO-66 MOF scaffolds for drug loading. Furthermore, folic

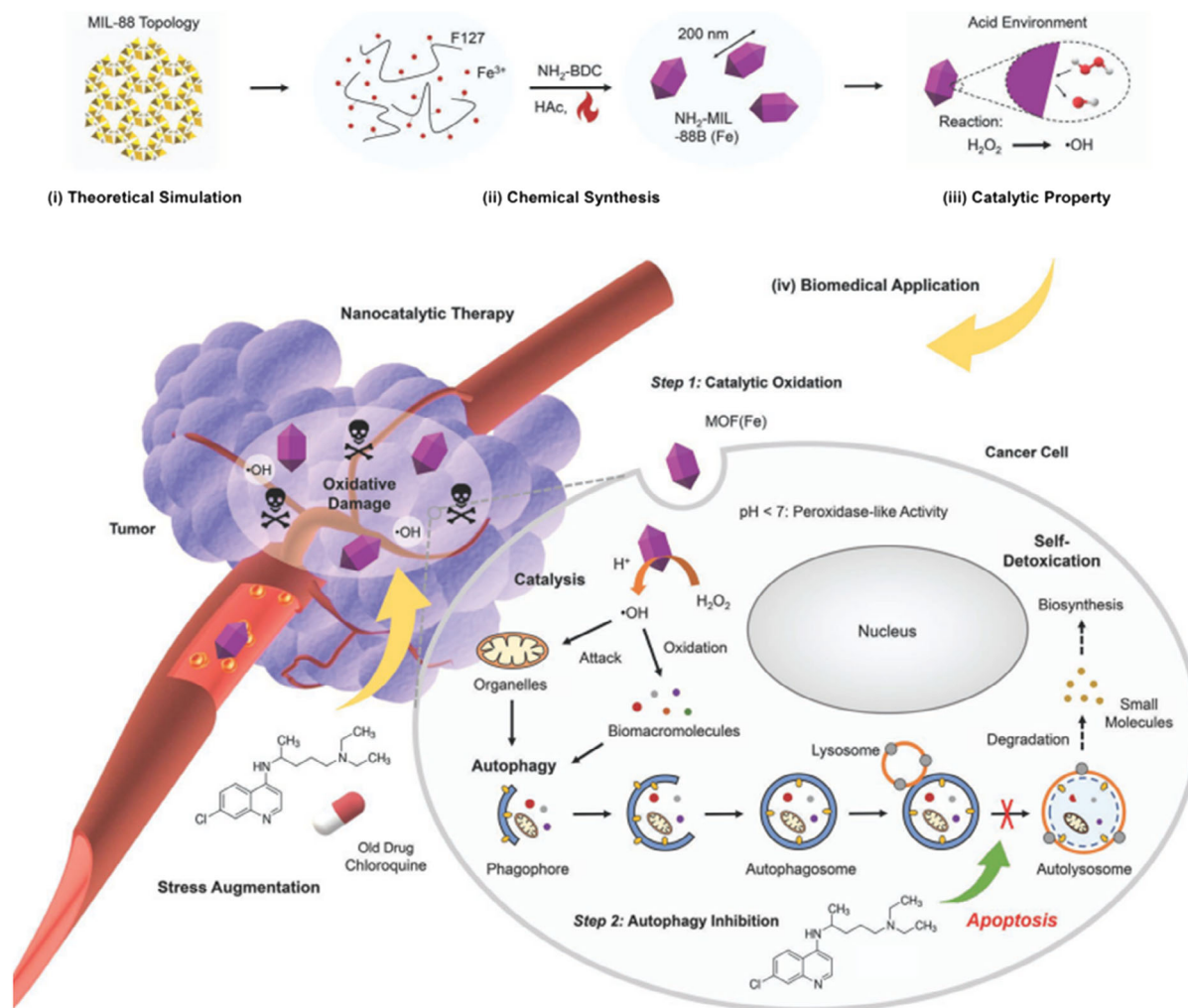


Figure 10. An MOF(Fe) nanocatalyst served as a pharmacological autophagy inhibitor that augmented ROS oxidation damage by generating a large amount of oxidizing $\cdot\text{OH}$ radicals in cancer cells. Reproduced with permission.^[146] Copyright 2020, Wiley-VCH.

acid-conjugated polyethyleneimine (PEI-Fa) was conjugated on the surface to act as a targeting entity. Upon irradiation at 808 nm, the PTT effects arising from the core polypyrrole NPs enhanced the release of chemodrugs for tumor treatment.

3.2. pH/Temperature-Responsive MOFs

Through a strategy of surface modification, Nagata and co-workers reported dual pH- and thermo-responsive stimuli for the controlled release of drugs by a MOF.^[155] The MOF was modified by a copolymer of N-isopropyl acrylamide (NIPAM) and acrylic acid (AA) in a postsynthetic process. The polymer displayed dual responsiveness by allowing the release of guest molecules (procainamide) from the MOF in an on-off manner. The polymer displayed quick release of guest molecules at pH 6.8 or a temperature lower than 25 °C, and release was suppressed at pH 4 or a temperature higher than 40 °C, as expected for both pH and thermosensitivity. This dual stimuli MOF shows potential for applications in cell imaging and demonstrates significant possibilities for controlled drug delivery.

3.3. pH/NIR-Responsive MOF

The combination of pH and NIR is a common strategy to improve the precise treatment efficiency, especially in cancer cells. Using these two stimuli, drug release and cell death could be manipulated at the targeted site. Jiang et al. reported a combinational therapy using quercetin and CuS NPs.^[156] The nano-system showed uniform morphology with spherical size, and the loading of quercetin was high and exhibited NIR-induced release behavior and pH responsiveness. Specifically, the drawbacks due to bioavailability, drug chemical instability, and low solubility in water were considerably overcome by the designed folic acid—bovine serum albumin (FA-BSA)/CuS@ZIF-8 DDS. The quercetin chemical study demonstrated improvement with the application of drug carriers. FA-BSA-modified MOF enhanced tumor cell cellular uptake, as demonstrated by in vivo and in vitro studies. The nanocomposite displayed toxicity and a low hemolysis ratio relative to normal organs, and it was safely administered intravenously. The in vivo and in vitro studies demonstrated that this system had a radiation-induced anticancer

effect better than those of PPT or chemotherapy alone, which displayed significantly enhanced tumor growth.

3.4. pH/Redox-Responsive MOF

Ren et al. developed pH- and redox-responsive ZIF-8@DOX@organo-silica (ZDOS) NPs with disulfide bridges, which facilitated degradation upon treatment by reducing agents.^[157] The synthesized ZDOS NPs displayed a good DOX loading capacity with redox and pH dual delivery properties. The release of DOX into tumor cells by DOX-loaded vesicles and total intracellular DOX delivery due to the high concentration of GSH and low pH led to a deconstruction of particles and enhanced cytotoxicity of DOX for cancer cells. The particles passed into cells primarily by endocytosis and were localized in lysosomal compartments. Compared with free DOX, the ZDOS NPs showed high potential and enhanced anticancer efficiencies, as proven by *in vivo* studies.

Zhou et al. reported a ZIF-8-coated ABA-type diselenide-containing triblock copolymer (PEG-PUSeSe-PEG) DDS.^[158] ZIF-8 served as a gatekeeper to delay drug release from the particles. Furthermore, in the presence of pH and redox stimuli, the drug (DOX)-loaded nanomaterial exhibited dual-responsive delivery *in vitro*. DOX delivery from the nanocomposite at pH 7.4 was inhibited, and only 21.1% was released in 24 h due to the blocking effect of ZIF-8 triggered by GSH. Moreover, the accelerated release at pH 5.0 increased to 81.2% and was 100% at pH 4.2, displaying the pH-responsive property of the ZIF-8 shell. When triggered by H₂O₂ or a low concentration of redox agent, the same release was noticed. A similar pH- and redox-responsive MIL-101 was also reported by Wang et al. for tumor-targeted DDSs.^[159] *In vitro* and *in vivo* studies demonstrated that a synthesized MOF loaded with DOX caused effective tumor suppression.

3.5. ATP/pH-Responsive MOF

Another interesting dual MOF reported by Jiang et al. was ZIF-90, which was synthesized via a fast assembly process.^[160] Compared with ZIF-8, ZIF-90 exhibited targeting ability for mitochondria and good cell biocompatibility. To prove the utility of ZIF-90 in the treatment of cancer *in vivo*, ZIF-90 was loaded with DOX and conjugated to Y1 receptor ligands for tumor targeting. The modified ZIF-90 decreased the premature release of DOX and more effectively triggered release inside cancer cells with low pH and higher adenosine triphosphate levels. After 40 days of treatment, the combined DOX release and dual-responsive delivery proved the efficacy of DOX-loaded ZIF-90 in cancer cells, displaying an 80% survival rate. This ZIF-90 could be used for promising triple-negative breast cancer treatment.

4. Conclusions

MOF-based particles have been extensively developed as effective platforms for on-demand DDSs by tumor therapeutics. Furthermore, there have been many studies exhibiting success in *in vitro* and *in vivo* cancer therapy by applying MOF-based DDSs as pH-responsive, PTT, PDT, or redox agents with further applications in chemotherapy and bioimaging. Recently, highly

functionalized MOF-based composites and new treatment approaches to enhance the efficacy of combination therapies have been proposed for further evaluation. Moreover, the Fenton reaction or nanocatalytic medicines induced by MOFs have been applied to elicit immune responses for further immune therapy. Despite the recent excitement regarding tumor therapy, several issues for translation of MOF into the clinic need to be further addressed in the future. First, on-demand drug release has been mainly dominated by the tumor microenvironment; therefore, blood flow, pH variation, oxygenation, changes in microenvironments or tumor heterogeneity might decrease the responsive efficacy, leading to insufficient drug release. In addition, abnormal tumor vasculature has a critical impact on tumor progression. In this regard, delivery of oxygen or nitric oxide with an MOF would potentially promote tumor vessel normalization, improving anticancer therapies. The on-demand release of gas regulates angiogenesis and vascular homeostasis.

Second, the accumulation of MOFs at the targeted site has been limited due to the recognition of the innate immune system, which potentially recognizes MOFs as foreign matter and clears them with the reticuloendothelial or mononuclear phagocyte system. The MOF accumulated in the liver and spleen could cause severe side effects during decomposition. A previous study applied polyethylene glycol (PEG) to reduce nonspecific interactions and suppress reticuloendothelial system (RES) uptake during circulation. However, excessively dosed PEGylated NPs usually cause immune rejection via the production of anti-PEG immunoglobulin M (IgM) antibodies. Therefore, biomimetic membranes such as red blood cells (RBCs), exosomes or macrophages on the MOF might be developed to prolong the blood circulation lifetime and decrease nonspecific macrophage uptake. For example, RBC membranes have a transmembrane protein (CD47) that signals the phagocyte receptor CD172a and inhibits the immune response.

To translate the MOF DDS to industrial applications, potent challenges must be addressed. The clinical issues of MOFs include biological problems, scale-up of manufacturing, biosafety, regulations, and cost utility. In addition, the next generation of MOFs latently exhibits specific targeting capability and specific inhibition of tumors but has to overcome the barriers of clinical trials, including identification of targeting biomarkers and precise conjugation. Further work may also be concentrated on the development of stable and low-toxicity MOF carriers by choosing functionalized MOFs with bioactive substances to decrease toxic effects. Theranostic MOFs present a time-honored challenge in biomedical advancement. Looking forward to optimistic advancements for clinical applications of MOFs will be made.

Acknowledgements

This work was financially supported by the Ministry of Science and Technology of the Republic of China, Taiwan under contracts MOST 109-2636-E-007-014 and MOST 108-2636-E-007-001 and by National Tsing Hua University (109Q2507E1) in Taiwan.

Conflict of Interest

The authors declare no conflict of interest.

Keywords

controlled release, drug delivery, metal-organic frameworks, nanomedicines, tumor therapies

Received: January 13, 2021

Revised: March 26, 2021

Published online:

- [1] L. Feng, K. Y. Wang, G. S. Day, H. C. Zhou, *Chem. Soc. Rev.* **2019**, *48*, 4823.
- [2] D. Shao, F. Zhang, F. Chen, X. Zheng, H. Hu, C. Yang, Z. Tu, Z. Wang, Z. Chang, J. Lu, T. Li, Y. Zhang, L. Chen, K. W. Leong, W. Dong, *Adv. Mater.* **2020**, *32*, 2004385.
- [3] S. Y. Sung, Y. L. Su, W. Cheng, P. F. Hu, C. S. Chiang, W. T. Chen, S. H. Hu, *Nano Lett.* **2019**, *19*, 69.
- [4] Y. Barenholz, *J. Control. Release* **2012**, *160*, 117.
- [5] A. J. Montero, B. Adams, C. M. Diaz-Montero, S. Glück, *Expert Rev. Clin. Pharmacol.* **2011**, *4*, 329.
- [6] M. S. Angst, D. R. Drover, *Clin. Pharmacokinet.* **2006**, *45*, 1153.
- [7] P. A. Dinndorf, J. Gootenberg, M. H. Cohen, P. Keegan, R. Pazdur, *Oncologist* **2007**, *12*, 991.
- [8] R. Freund, U. Lächelt, T. Gruber, B. Rühle, S. Wuttke, *ACS Nano* **2018**, *12*, 2094.
- [9] R. S. Hsu, J. H. Fang, W. T. Shen, Y. C. Sheu, C. K. Su, W. H. Chiang, S. H. Hu, *Nanoscale* **2020**, *12*, 11153.
- [10] M. R. Chiang, Y. L. Su, C. Y. Chang, C. W. Chang, S. H. Hu, *Mater. Horiz.* **2020**, *7*, 1051.
- [11] J. Liu, Z. Guo, Y. Li, J. Liang, J. Xue, J. Xu, J. M. Whitelock, L. Xie, B. Kong, K. Liang, *Adv. NanoBiomed. Res.* **2020**, *1*, 2000034.
- [12] Y. L. Su, L. W. Kuo, C. H. Hsu, C. S. Chiang, Y. J. Lu, S. J. Chang, S. H. Hu, *J. Control Release* **2020**, *321*, 159.
- [13] Y. L. Su, K. T. Chen, Y. C. Sheu, S. Y. Sung, R. S. Hsu, C. S. Chiang, S. H. Hu, *ACS Nano* **2016**, *10*, 9420.
- [14] R. Freund, U. Lächelt, T. Gruber, B. Rühle, S. Wuttke, *ACS Nano* **2018**, *12*, 2094.
- [15] B. F. Hoskins, R. Robson, *J. Am. Chem. Soc.* **1989**, *111*, 5962.
- [16] R. S. Forgan, *Chem. Sci.* **2020**, *11*, 4546.
- [17] A. Schneemann, V. Bon, I. Schwedler, I. Senkovska, S. Kaskel, R. A. Fischer, *Chem. Soc. Rev.* **2014**, *43*, 6062.
- [18] C. Vaitsis, G. Sourkouni, C. Argiris, *Ultrasonics Sonochem.* **2019**, *52*, 106.
- [19] O. M. Yaghi, M. O. Keeffe, N. W. Ockwig, H. K. Chae, M. Eddaoudi, J. Kim, *Nature* **2003**, *423*, 705.
- [20] S. Yuan, J. S. Qin, C. T. Lollar, H. C. Zhou, *ACS Cent. Sci.* **2018**, *4*, 440.
- [21] A. E. Baumann, D. A. Burns, B. Liu, V. S. Thoi, *Commun. Chem.* **2019**, *2*, 86.
- [22] H. C. Zhou, J. R. Long, O. M. Yaghi, *Chem. Rev.* **2012**, *112*, 673.
- [23] C. Gropp, S. Canossa, S. Wuttke, F. Gándara, Q. Li, L. Gagliardi, O. M. Yaghi, *ACS Cent. Sci.* **2020**, *6*, 1255.
- [24] Z. Ji, H. Wang, S. Canossa, S. Wuttke, O. M. Yaghi, *Adv. Funct. Mater.* **2020**, *30*, 2000238.
- [25] R. S. Forgan, *Dalton Trans.* **2019**, *48*, 9037.
- [26] R. J. Marshall, R. S. Forgan, *Eur. J. Inorg. Chem.* **2016**, *27*, 4310.
- [27] V. F. Samanidou, E. A. Deliyanni, *Molecules* **2020**, *25*, 960.
- [28] I. Kurzydym, I. Czekaj, *Tech. Trans.* **2020**, e2020012.
- [29] T. Chalati, P. Horcajada, P. Couvreur, C. Serre, M. B. Yahia, G. Maurin, R. Gref, *Nanomedicine* **2011**, *6*, 1683.
- [30] S. Mangal, S. S. Priya, *MRS Energy Sustain.* **2020**, *38*, 169.
- [31] P. Silva, S. M. F. Vilela, J. P. C. Tomé, F. A. Almeida Paz, *Chem. Soc. Rev.* **2015**, *44*, 6774.
- [32] Y. Wang, J. Yan, N. Wen, H. Xiong, S. Cai, Q. He, Y. Hu, D. Peng, Z. Liu, Y. Liu, *Biomaterials* **2020**, *230*, 119619.
- [33] M. X. Wu, Y. W. Yang, *Adv. Mater.* **2017**, *29*, 1606134.
- [34] Q. Jia, Z. Li, C. Guo, X. Huang, Y. Song, N. Zhou, M. Wang, Z. Zhang, L. He, M. Du, *Nanoscale* **2019**, *11*, 20956.
- [35] D. Wang, J. Zhou, R. Chen, R. Shi, G. Zhao, G. Xia, R. Li, Z. Liu, J. Tian, H. Wang, Z. Guo, H. Wang, Q. Chen, *Biomaterials* **2016**, *100*, 27.
- [36] S. Javanbakht, A. Hemmati, H. Namazi, A. Heydari, *Int. J. Biol. Macromol.* **2020**, *155*, 876.
- [37] R. Zhang, Y. Xu, Y. Zhang, H. S. Kim, A. Sharma, J. Gao, G. Yang, J. S. Kim, Y. Sun, *Chem. Sci.* **2019**, *10*, 8348.
- [38] A. R. Chowdhuri, T. Singh, S. K. Ghosh, S. K. Sahu, *ACS Appl. Mater. Interfaces* **2016**, *8*, 16573.
- [39] R. Röder, T. Preiß, P. Hirschle, B. Steinborn, A. Zimpel, M. Höhn, J. O. Rädler, T. Bein, E. Wagner, S. Wuttke, U. Lächelt, *J. Am. Chem. Soc.* **2017**, *139*, 2359.
- [40] K. Xing, R. Fan, F. Wang, H. Nie, X. Du, S. Gai, P. Wang, Y. Yang, *ACS Appl. Mater. Interfaces* **2018**, *26*, 2274.
- [41] R. Abazari, A. R. Mahjoub, F. Ataei, A. Morsali, C. L. C. Warren, K. Mehdizadeh, A. M. Z. Slawin, *Inorg. Chem.* **2018**, *57*, 13364.
- [42] Y. Yang, Q. Hu, Q. Zhang, K. Jiang, W. Lin, Y. Yang, Y. Cui, G. Qian, *Mol. Pharmaceutics* **2016**, *13*, 2782.
- [43] Y. D. Zhu, S. P. Chen, H. Zhao, Y. Yang, X. Q. Chen, J. Sun, H. S. Fan, X. D. Zhang, *ACS Appl. Mater. Interfaces* **2016**, *8*, 34209.
- [44] T. Xue, C. Xu, Y. Wang, Y. Wang, H. Tian, Y. Zhang, *Biomater. Sci.* **2019**, *7*, 4615.
- [45] A. Lajevardi, M. H. Sadr, A. Badiei, M. Armaghan, *J. Mol. Liq.* **2020**, *307*, 112996.
- [46] A. Botet-Carreras, C. Tamames-Tabar, F. Salles, S. Rojas, E. Imbuluzqueta, H. Lana, M. J. Blanco-Prieto, P. Horcajada, *J. Mater. Chem. B* **2021**, *9*, 2233.
- [47] A. G. Márquez, T. Hidalgo, H. Lana, D. Cunha, M. J. Blanco-Prieto, C. Álvarez-Lorenzo, C. Boissière, C. Sánchez, C. Serrea, P. Horcajada, *J. Mater. Chem. B* **2016**, *4*, 7031.
- [48] Z. Liu, T. Li, F. Han, Y. Gan, Y. Wang, J. Shi, T. Wang, M. L. Akhtar, Y. Li, *Biomater. Sci.* **2019**, *7*, 3683.
- [49] D. Ling, H. Li, W. Xi, Z. Wang, A. Bednarkiewicz, S. T. Dibaba, L. Shi, L. Sun, *J. Mater. Chem. B* **2020**, *8*, 1316.
- [50] H. Zheng, Y. Zhang, L. Liu, W. Wan, P. Guo, A. M. Nyström, X. Zou, *J. Am. Chem. Soc.* **2015**, *138*, 962.
- [51] M. Q. Tolentino, A. K. Hartmann, D. T. Loe, J. L. Rouge, *J. Mater. Chem. B* **2020**, *8*, 5637.
- [52] L. Zhang, Y. Gao, S. Sun, Z. Li, A. Wu, L. Zeng, *J. Mater. Chem.* **2020**, *8*, 1739.
- [53] Y. T. Qin, H. Peng, X. W. He, W. Y. Li, Y. K. Zhang, *ACS Appl. Mater. Interfaces* **2019**, *11*, 34268.
- [54] W. L. Jiang, Q. J. Fu, B. J. Yao, L. G. Ding, C. X. Liu, Y. B. Dong, *ACS Appl. Mater. Interfaces* **2017**, *9*, 36438.
- [55] F. Duan, X. Feng, X. Yang, W. Sun, Y. Jin, H. Liu, K. Ge, Z. Li, J. Zhang, *Biomaterials* **2017**, *122*, 23.
- [56] T. Simon-Yarza, M. Giménez-Marqués, R. Mrimi, R. Gref, P. Horcajada, C. Serre, P. Couvreur, *Angew. Chem., Int. Ed.* **2017**, *56*, 15565.
- [57] Y. Jin, Y. Wang, J. Yang, H. Zhang, Y. W. Yang, W. Chen, W. Jiang, J. Qu, Y. Guo, B. Wang, *Cell Rep. Phys. Sci.* **2020**, *1*, 100173.
- [58] H. Chen, J. Yang, L. Sun, H. Zhang, Y. Guo, J. Qu, W. Jiang, W. Chen, J. Ji, Y. W. Yang, B. Wang, *Small* **2019**, *15*, 1903880.
- [59] P. Markopoulou, N. Panagiotou, A. Li, R. Bueno-Perez, D. Madden, S. Buchanan, D. Fairen-Jimenez, P. G. Shiels, R. S. Forgan, *Cell Rep. Phys. Sci.* **2020**, *1*, 100254.
- [60] E. Ploetz, A. Zimpel, V. Cauda, D. Bauer, D. C. Lamb, C. Haisch, S. Zahler, A. M. Vollmar, S. Wuttke, H. Engelke, *Adv. Mater.* **2020**, *32*, 1907267.

- [61] S. Wang, M. Wahiduzzaman, L. Davis, A. Tissot, W. Shepard, J. Marrot, C. Martineau-Corcos, D. Hamdane, G. Maurin, S. Devautour-Vinot, C. Serre, *Nat. Commun.* **2018**, *9*, 4937.
- [62] R. J. Marshall, Y. Kalinovsky, S. L. Griffin, C. Wilson, B. A. Blight, R. S. Forgan, *J. Am. Chem. Soc.* **2017**, *139*, 6253.
- [63] S. M. F. Vilela, P. Salcedo-Abraira, I. Colinet, F. Salles, M. C. de Koning, M. J. A. Joosen, C. Serre, P. Horcajada, *Nanomaterials* **2017**, *7*, 321.
- [64] E. Bellido, M. Guillevic, T. Hidalgo, M. J. S. Ortega, C. Serre, P. Horcajada, *Langmuir* **2014**, *30*, 591.
- [65] Z. Dong, Y. Sun, J. Chu, X. Zhang, H. Deng, *J. Am. Chem. Soc.* **2017**, *139*, 14209.
- [66] H. Furukawa, K. E. Cordova, M. O'Keeffe, O. M. Yaghi, *Science* **2013**, *341*, 1230444.
- [67] M. X. Wu, J. Gao, F. Wang, J. Yang, N. Song, X. Jin, P. Mi, J. Tian, J. Luo, F. Liang, Y. W. Yang, *Small* **2018**, *14*, 1704440.
- [68] W. T. Shen, R. S. Hsu, J. H. Fang, P. F. Hu, C. S. Chiang, S. H. Hu, *Nano Lett.* **2021**, *3*, 1375.
- [69] W. Lin, Y. Cui, Y. Yang, Q. Hu, G. Qian, *Dalton Trans.* **2018**, *47*, 15882.
- [70] K. Jiang, L. Zhang, Q. Hu, Q. Zhang, W. Lin, Y. Cui, Y. Yang, G. Qian, *Chem. Eur. J.* **2017**, *23*, 10215.
- [71] D. Zheng, P. Yu, Z. Wei, C. Zhong, M. Wu, X. Liu, *Nano-Micro Lett.* **2020**, *12*, 94.
- [72] Q. Wang, D. Astruc, *Chem. Rev.* **2020**, *120*, 1438.
- [73] H. Babaei, M. E. DeCoster, M. Jeong, Z. M. Hassan, T. Islamoglu, H. Baumgart, A. J. H. McGaughey, E. Rede, O. K. Farha, P. E. Hopkins, J. A. Malen, C. E. Wilmer, *Nat. Commun.* **2020**, *11*, 4010.
- [74] E. A. Dolgoplova, A. J. Brandt, O. A. Ejegbavwo, A. S. Duke, T. D. Maddumapatabandi, R. P. Galhenage, B. W. Larson, O. G. Reid, S. C. Ammal, A. Heyden, M. Chandrashekar, V. Stavila, D. A. Chen, N. B. Shustova, *J. Am. Chem. Soc.* **2017**, *139*, 5201.
- [75] S. Kampouri, C. P. Ireland, B. Valizadeh, E. Oveisi, P. A. Schouwink, M. Mensi, K. C. Stylianou, *ACS Appl. Energy Mater.* **2018**, *1*, 6541.
- [76] Q. Li, Y. Pan, H. Li, L. Alhalhooly, Y. Li, B. Chen, Y. Choi, Z. Yang, *ACS Appl. Mater. Interfaces* **2020**, *12*, 41794.
- [77] M. D. Wang, G. C. Gong, J. Feng, T. Wang, C. D. Ding, B. Zhou, W. Jiang, J. Fu, *ACS Appl. Mater. Interfaces* **2016**, *8*, 23289.
- [78] F. Z. Jin, C. C. Zhao, H. C. Ma, G. J. Chen, Y. B. Dong, *Inorg. Chem.* **2019**, *58*, 9253.
- [79] G. Tana, Y. Zhong, L. Yang, Y. Jiang, J. Liu, F. Rena, *Chem. Eng. J.* **2020**, *390*, 124446.
- [80] A. Karmakar, P. G. M. Mileo, I. Bok, S. B. Peh, J. Zhang, H. Yuan, G. Maurin, D. Zhao, *Angew. Chem., Int. Ed.* **2020**, *132*, 11096.
- [81] S. Nagata, K. Kokado, K. Sada, *Chem. Commun.* **2015**, *51*, 8614.
- [82] W. X. Lin, Q. Hu, J. C. Yu, K. Jiang, Y. Y. Yang, S. C. Xiang, Y. J. Cui, Y. Yang, Z. Y. Wang, G. D. Qian, *ChemPlusChem* **2016**, *81*, 804.
- [83] S. Dai, F. Nouar, S. Zhang, A. Tissot, C. Serre, *Angew. Chem., Int. Ed.* **2021**, *60*, 4282.
- [84] S. Wang, T. Kitao, N. Guillou, M. Wahiduzzaman, C. Martineau-Corcos, F. Nouar, A. Tissot, L. Binet, N. Ramsahye, S. Devautour-Vinot, S. Kitagawa, S. Seki, Y. Tsutsui, V. Briois, N. Steunou, G. Maurin, T. Uemura, C. Serre, *Nat. Commun.* **2018**, *9*, 1660.
- [85] S. Wang, J. S. Lee, M. Wahiduzzaman, J. Park, M. Muschi, C. Martineau-Corcos, A. Tissot, K. H. Cho, J. Marrot, W. Shepard, G. Maurin, J. S. Chang, C. Serre, *Nat. Energy* **2018**, *3*, 985.
- [86] L. N. McHugh, M. J. McPherson, L. J. McCormick, S. A. Morris, P. S. Wheatley, S. J. Teat, D. McKay, D. M. Dawson, C. E. F. Sansome, S. E. Ashbrook, C. A. Stone, M. W. Smith, R. E. Morris, *Nat. Chem.* **2018**, *10*, 1096.
- [87] F. Himeur, I. Stein, D. S. Wragg, A. M.Z. Slawin, P. Lightfoot, R. E. Morris, *Solid State Sci.* **2010**, *12*, 418.
- [88] E. R. Parnham, R. E. Morris, *Acc. Chem. Res.* **2007**, *40*, 1005.
- [89] H. Zhang, X. T. Tian, Y. Shang, Y. H. Li, X. B. Yin, *ACS Appl. Mater. Interfaces* **2018**, *10*, 28390.
- [90] J. Yao, Y. Liu, J. Wang, Q. Jiang, D. She, H. Guo, N. Sun, Z. Pang, C. Deng, W. Yang, S. Shen, *Biomaterials* **2019**, *195*, 51.
- [91] M. Giménez-Marqués, A. Santiago-Portillo, S. Navalón, M. Álvaro, V. Briois, F. Nouar, H. Garcia, C. Serre, *J. Mater. Chem. A*, **2019**, *7*, 20285.
- [92] T. Hidalgo, M. Alonso-Nocelo, B. L. Bouzo, S. Reimondez-Troitiño, C. Abuin-Redondo, M. de la Fuente, P. Horcajada, *Nanoscale* **2020**, *12*, 4839.
- [93] W. Morris, W. E. Briley, E. Auyeung, M. D. Cabezas, C. A. Mirkin, *J. Am. Chem. Soc.* **2014**, *136*, 7261.
- [94] S. Haddad, I. A. Lázaro, M. Fantham, A. Mishra, J. Silvestre-Albero, J. W. M. Osterrieth, G. S. K. Schierle, C. F. Kaminski, R. S. Forgan, D. Fairen-Jimenez, *J. Am. Chem. Soc.* **2020**, *142*, 6661.
- [95] L. Huang, J. Cai, M. He, B. Chen, B. Hu, *Ind. Eng. Chem. Res.* **2018**, *57*, 6201.
- [96] A. Pinna, R. Ricco', R. Migheli, G. Rocchitta, P. A. Serra, P. Falcaro, L. Malfatti, P. Innocenzi, *RSC Adv.* **2018**, *8*, 25664.
- [97] Z. Xiang, Y. Qi, Y. Lu, Z. Hu, X. Wang, W. Jia, J. Hu, J. Ji, W. Lu, *J. Mater. Chem. B* **2020**, *8*, 8671.
- [98] L. He, Q. Ni, J. Mu, W. Fan, L. Liu, Z. Wang, L. Li, W. Tang, Y. Liu, Y. Cheng, L. Tang, Z. Yang, Y. Liu, J. Zou, W. Yang, O. Jacobson, F. Zhang, P. Huang, X. Chen, *J. Am. Chem. Soc.* **2020**, *142*, 6822.
- [99] X. Y. Xu, C. Chu, H. Fu, X. D. Du, P. Wang, W. Zheng, C. C. Wang, *Chem. Eng. J.* **2018**, *350*, 436.
- [100] A. Cadiou, N. Kolobov, S. Srinivasan, M. G. Goesten, H. Haspel, A. V. Bavykina, M. R. Tchalala, P. Maity, A. Goryachev, A. S. Poryvaev, M. Eddaoudi, M. V. Fedin, O. F. Mohammed, J. Gascon, *Angew. Chem., Int. Ed.* **2020**, *59*, 13468.
- [101] N. Prasetya, B. C. Donose, B. P. Ladewig, *J. Mater. Chem. A* **2018**, *6*, 16390.
- [102] Y. Zhong, Y. Mao, S. Shi, M. Wan, C. Ma, S. Wang, C. Chen, D. Zhao, N. Zhang, *ACS Appl. Mater. Interfaces* **2019**, *11*, 32251.
- [103] F. Ke, Y. P. Yuan, L. G. Qiu, Y. H. Shen, A. J. Xie, J. F. Zhu, X. Y. Tian, L. D. Zhang, *J. Mater. Chem.* **2011**, *21*, 3843.
- [104] D. Yang, G. Yang, S. Gai, F. He, G. An, Y. Dai, R. Lv, P. Yang, *Nanoscale* **2015**, *7*, 19568.
- [105] Z. Xue, M. Zhu, Y. Dong, T. Feng, Z. Chen, Y. Feng, Z. Shan, J. Xu, S. Meng, *Nanoscale* **2019**, *11*, 11709.
- [106] M. D. Rowe, D. H. Thamrn, S. L. Kraft, S. G. Boyes, *Biomacromolecules* **2009**, *10*, 983.
- [107] R. Haldar, L. Heinke, C. Wöll, *Adv. Mater.* **2020**, *32*, 1905227.
- [108] M. Lismont, L. Dreesen, S. Wuttke, *Adv. Funct. Mater.* **2017**, *27*, 1606314.
- [109] W. Zhang, J. Lu, X. Gao, P. Li, W. Zhang, Y. Ma, H. Wang, B. Tang, *Angew. Chem., Int. Ed.* **2018**, *130*, 4985.
- [110] X. Cai, Z. Xie, B. Ding, S. Shao, S. Liang, M. Pang, J. Lin, *Adv. Sci.* **2019**, *6*, 1900848.
- [111] D. Xu, Y. You, F. Zeng, Y. Wang, C. Liang, H. Feng, X. Ma, *ACS Appl. Mater. Interfaces* **2018**, *10*, 15517.
- [112] J. L. Li, B. Tang, B. Yuan, L. Sun, X. G. Wang, *Biomaterials* **2013**, *34*, 9519.
- [113] J. R. Melamed, R. S. Edelstein, E. S. Day, *ACS Nano* **2015**, *9*, 6.
- [114] W. Cai, H. Gao, C. Chu, X. Wang, J. Wang, P. Zhang, G. Lin, W. Li, G. Liu, X. Chen, *ACS Appl. Mater. Interfaces* **2017**, *9*, 2040.
- [115] F. Jia, G. Li, B. Yang, B. Yu, Y. Shen, H. Cong, *Nanotechnol. Rev.* **2019**, *8*, 2191.
- [116] S. Y. Yin, G. Song, Y. Yang, Y. Zhao, P. Wang, L. M. Zhu, X. Yin, X. B. Zhang, *Adv. Funct. Mater.* **2019**, *29*, 1901417.
- [117] X. Zeng, S. Yan, P. Chen, W. Du, B. F. Liu, *Nano. Res.* **2019**, *13*, 1527.
- [118] X. Fu, Z. Yang, T. Deng, J. Chen, Y. Wen, X. Fu, L. Zhou, Z. Zhu, C. Yu, *J. Mater. Chem. B*, **2019**, *8*, 1481.

- [119] D. Wang, J. Zhou, R. Chen, R. Shi, G. Zhao, G. Xia, R. Li, Z. Liu, J. Tian, H. Wang, Z. Guo, H. Wang, Q. Chen, *Biomaterials* **2016**, *107*, 88.
- [120] H. B. Zheng, H. H. Chen, Y. L. Wang, P. Z. Gao, X. P. Liu, E. V. Rebrov, *ACS Appl. Mater. Interfaces* **2020**, *12*, 45987.
- [121] X. Chen, M. Zhang, S. Li, L. Li, L. Zhang, T. Wang, M. Yu, Z. Moua, C. Wang, *J. Mater. Chem. B* **2017**, *5*, 1772.
- [122] Z. Fan, H. Liu, Y. Xue, J. Lin, Y. Fu, Z. Xia, D. Pan, J. Zhang, K. Qiao, Z. Zhang, Y. Liao, *Bioact. Mater.* **2021**, *6*, 312.
- [123] H. A. Schwartz, S. Olthof, D. Schaniel, K. Meerholz, U. Ruschewitz, *Inorg. Chem.* **2017**, *56*, 13100.
- [124] M. Dan-Hardi, C. Serre, T. Frot, L. Rozes, G. Maurin, C. Sanchez, G. Férey, *J. Am. Chem. Soc.* **2009**, *131*, 10857.
- [125] Y. Qin, J. Fan, W. Yang, B. Shen, Y. Yang, Q. Zhou, W. Chen, M. Daniyal, F. Xiao, W. B. Sheng, H. Yu, J. Zhou, W. Wang, C. Tong, B. Liu, *Anal. Chem.* **2020**, *92*, 1988.
- [126] X. Guo, Y. Cheng, X. Zhao, Y. Luo, J. Chen, W. E. Yuan, *J. Nanobiotechnol.* **2018**, *16*, 74.
- [127] Y. Miao, X. Zhao, Y. Qiu, Z. Liu, W. Yang, X. Jia, *ACS Appl. Bio Mater.* **2019**, *2*, 895.
- [128] C. Arias-Duque, E. Bladt, M. A. Muñoz, J. C. Hernández-Garrido, M. A. Cauqui, J. M. Rodríguez-Izquierdo, G. Blanco, S. Bals, J. J. Calvino, J. A. Pérez-Omil, M. P. Yeste, *Chem. Mater.* **2017**, *29*, 9340.
- [129] J. Zhao, Y. Yang, X. Han, C. Liang, J. Liu, X. Song, Z. Liu Zili Ge, *ACS Appl. Mater. Interfaces* **2017**, *9*, 23555.
- [130] B. Lei, M. Wang, Z. Jiang, W. Qi, R. Su, Z. He, *ACS Appl. Mater. Interfaces* **2018**, *10*, 16698.
- [131] C. Liu, X. Xu, J. Zhou, J. Yan, D. Wang, H. Zhang, *BMC Mater.* **2020**, *2*, 7.
- [132] A. M. Hussain, Y. L. Huang, K. J. Pan, I. A. Robinson, X. Wang, E. D. Wachsman, *ACS Appl. Mater. Interfaces* **2020**, *12*, 18526.
- [133] T. Du, H. Zhang, J. Ruan, H. Jiang, H. Y. Chen, X. Wang, *ACS Appl. Mater. Interfaces* **2018**, *10*, 12417.
- [134] S. S. Wan, Q. Cheng, X. Zeng, X. Z. Zhang, *ACS Nano* **2019**, *13*, 6561.
- [135] S. Lee, J. T. Muya, H. Chung, J. Chang, *ACS Appl. Mater. Interfaces* **2019**, *11*, 43659.
- [136] W. H. Chen, G. F. Luo, M. Vázquez-González, R. Cazelles, Y. S. Sohn, R. Nechushtai, Y. Mandel, I. Willner, *ACS Nano* **2018**, *12*, 7538.
- [137] W. Lee, B. W. Kwon, Y. Kwon, *ACS Appl. Mater. Interfaces* **2018**, *10*, 36882.
- [138] T. Wang, S. Li, Z. Zou, L. Hai, X. Yang, X. Jia, A. Zhang, D. He, X. He, K. Wang, *J. Mater. Chem. B* **2018**, *6*, 3914.
- [139] Q. Li, Y. Pan, H. Li, L. Alhalhooly, Y. Li, B. Chen, Y. Choi, Z. Yang, *ACS Appl. Mater. Interfaces* **2020**, *12*, 41794.
- [140] J. Phipps, H. Chen, C. Donovan, D. Dominguez, S. Morgan, B. Weidman, C. Fan, M. H. Beyzavi, *ACS Appl. Mater. Interfaces* **2020**, *12*, 26084.
- [141] Y. Zhong, L. Yu, Q. He, Q. Zhu, C. Zhang, X. Cui, J. Zheng, S. Zhao, *ACS Appl. Mater. Interfaces* **2019**, *11*, 32769.
- [142] K. Kim, S. Lee, E. Jin, L. Palanikumar, J. H. Lee, J. C. Kim, J. S. Nam, B. Jana, T. H. Kwon, S. K. Kwak, W. Choe, J. H. Ryu, *ACS Appl. Mater. Interfaces* **2019**, *11*, 27512.
- [143] L. Wang, M. Huo, Y. Chen, J. Shi, *Adv. Healthcare Mater.* **2018**, *7*, 1701156.
- [144] W. Fan, N. Lu, P. Huang, Y. Liu, Z. Yang, S. Wang, G. Yu, Y. Liu, J. Hu, Q. He, J. Qu, T. Wang, X. Chen, *Angew. Chem., Int. Ed.* **2017**, *56*, 1229.
- [145] S. Dinda, S. Sarkar, P. K. Das, *Chem. Commun.* **2018**, *54*, 9929.
- [146] B. Yang, L. Ding, H. Yao, Y. Chen, J. Shi, *Adv. Mater.* **2020**, *32*, 1907152.
- [147] A. Fateeva, P. Horcajada, T. Devic, C. Serre, J. Marrot, J. M. Grenèche, M. Morcrette, J. M. Tarascon, G. Maurin, G. Férey, *Eur. J. Inorg. Chem.* **2010**, *2010*, 3789.
- [148] G. Férey, F. Millange, M. Morcrette, C. Serre, M. L. Doublet, J. M. Grenèche, J. M. Tarascon, *Angew. Chem., Int. Ed.* **2007**, *46*, 3259.
- [149] J. D. Evans, B. Garaia, H. Reinsch, W. Li, S. Dissegna, V. Bon, I. Senkovska, R. A. Fischer, S. Kaskel, C. Janiak, N. Stock, D. Volkmer, *Chem. Rev.* **2019**, *380*, 378.
- [150] Z. Li, N. Song, Y. W. Yang, *Matter* **2019**, *1*, 345.
- [151] L. L. Tan, H. Li, Y. C. Qiu, D. X. Chen, X. Wang, R. Y. Pan, Y. Wang, S. X. A. Zhang, B. Wang, Y. W. Yang, *Chem. Sci.* **2015**, *6*, 1640.
- [152] L. L. Tan, H. Li, Y. Zhou, Y. Zhang, X. Feng, B. Wang, Y. W. Yang, *Small* **2015**, *11*, 3807.
- [153] L. L. Tan, N. Song, S. X. A. Zhang, H. Li, B. Wang, Y. W. Yang, *J. Mater. Chem. B* **2016**, *4*, 135.
- [154] Y. Cheng, J. Yang, J. R. Wu, B. J. Gong, H. Y. Zhang, Y. W. Yang, *ACS Appl. Mater. Interfaces* **2018**, *10*, 34655.
- [155] S. Nagata, K. Kokado, K. Sada, *CrystEngComm* **2020**, *22*, 1106.
- [156] W. Jiang, H. Zhang, J. Wu, G. Zhai, Z. Li, Y. Luan, S. Garg, *ACS Appl. Mater. Interfaces* **2018**, *10*, 34513.
- [157] S. Z. Ren, D. Zhu, X. H. Zhu, B. Wang, Y. S. Yang, W. X. Sun, X. M. Wang, P. C. Lv, Z. C. Wang, H. L. Zhu, *ACS Appl. Mater. Interfaces* **2019**, *11*, 20678.
- [158] W. Zhou, L. Wang, F. Li, W. Zhang, W. Huang, F. Huo, H. Xu, *Adv. Funct. Mater.* **2017**, *27*, 1605465.
- [159] X. G. Wang, Z. Y. Dong, H. Cheng, S. S. Wan, W. H. Chen, M. Z. Zou, J. W. Huo, H. X. Deng, X. Z. Zhang, *Nanoscale* **2015**, *7*, 16061.
- [160] Z. Jiang, Y. Wang, L. Sun, B. Yuan, Y. Tian, L. Xiang, Y. Li, Y. Li, J. Lia, A. Wu, *Biomaterials* **2019**, *197*, 41.



Bhanu Nirosha Yalamandala received her Bachelor of Pharmacy from the Jawaharlal Nehru technological University Kakinada, India, and then obtained her Master of Pharmacy from the Acharya Nagarjuna University, Guntur, India. Currently, she is pursuing her Ph.D. in the Department of Biomedical Engineering and Environmental Sciences from National Tsing Hua University, Taiwan. Her research interests include MOF NPs for lung metastasis.



Wei-Ting Shen obtained his bachelor's in materials science and engineering from National Tsing Hua University, Taiwan (NTHU). He is currently pursuing master's from the Department of Biomedical Engineering and Environmental Sciences, NTHU. His main research interest focuses on utilizing designed NPs as agents or carriers with biological components for therapeutic use.



Sheng-Hao Min received his bachelor's in biomedical sciences and engineering from National Central University, Taiwan (NCU), with minors in chemicals and materials engineering. Currently, he is now pursuing for master's from Department of Biomedical Engineering and Environmental Sciences, National Tsing Hua University, Taiwan. His research focuses on designing functional NPs as a treating agent for lung-metastasis cancer.



Wen-Hsuan Chiang obtained his Ph.D. from Department of Chemical Engineering at National Chung Hsing University, in 2009. During 2010–2015, he conducted postdoctoral research in Department of Biomedical Engineering and Environmental Sciences at National Tsing Hua University. Now he is assistant professor at the Department of Chemical Engineering at National Chung Hsing University. His research interests include design of functionalized amphiphilic copolymer, stimuli-responsive polymeric NPs, drug delivery, and cancer therapy.



Shing-jyh Chang received the M.D. from the Taipei Medical University School of Medicine, Taipei, Taiwan, and Ph.D. in the Institute of Molecular and Cellular Biology from the National Tsing Hua University, Hsinchu Taiwan. Currently, he is a gynecology oncologist in Hsinchu MacKay Memorial Hospital, Hsinchu, Taiwan, and a joint associate professor in the Department of Medical Science, National Tsing Hua University, Hsinchu, Taiwan. His primary research interests are studying gynecological cancers and their carcinogenic mechanisms. Recently, he focused on cancer 3D modeling and drug screening strategy design.



Shang-Hsiu Hu (B.S.—chemical engineering—2004, NCHU; M.S.—materials—2006, NCTU; Ph.D.—materials—2010, NCTU) has been an associate professor at National Tsing Hua University since 2017 (Department of Biomedical and Environmental Sciences). His research explores novel nanomaterials and nanotechnologies to develop advanced drug and gene delivery systems with the promise to improve health care. He received NTHU Young Faculty Research Award (2015) and Prof. Chao-Ren Lee-Young Scholar Award (2015), Taiwan MOST Ta-You Wu Memorial Award (2017), MOST Young Scholar Fellowship (2018), and National Innovation Award (2019).